

# intRinsic: an R package for model-based estimation of the intrinsic dimension of a dataset

Francesco Denti  
fdenti@uci.edu  
University of California, Irvine

December 23, 2024

The estimation of the intrinsic dimension of a dataset is a fundamental step in most dimensionality reduction techniques. This article illustrates `intRinsic`, an R package that implements novel state-of-the-art likelihood-based estimators of the intrinsic dimension of a dataset. In detail, the methods included in this package are the `TWO-NN`, `Gride`, and `Hidalgo` models. To allow these novel estimators to be easily accessible, the package contains a few high-level, intuitive functions that rely on a broader set of efficient, low-level routines. `intRinsic` encompasses models that fall into two categories: homogeneous and heterogeneous intrinsic dimension estimators. The first category contains the `TWO-NN` and `Gride` models. The functions dedicated to these two methods carry out inference under both the frequentist and Bayesian frameworks. In the second category we find `Hidalgo`, a Bayesian mixture model, for which an efficient Gibbs sampler is implemented. After discussing the theoretical background, we demonstrate the performance of the models on simulated datasets. This way, we can assess the results by comparing them with the ground truth. Then, we employ the package to study the intrinsic dimension of the `Alon` dataset, obtained from a famous microarray experiment. We show how the estimation of homogeneous and heterogeneous intrinsic dimensions allows us to gain valuable insights about the topological structure of a dataset.

## 1 Introduction

Statisticians and data scientists are often called to manipulate, analyze, and summarize datasets that present high-dimensional and elaborate dependency structures. In multiple cases, these large datasets are constituted by variables that contain a considerable amount of redundant information. One can exploit these redundancies to represent a large dataset on a much lower-dimensional scale. This summarization procedure, called *dimensionality reduction*, is a fundamental step in many statistical analyses. For example, dimensionality

reduction techniques make otherwise prohibitive manipulation and visualization of large datasets feasible by reducing computational time and memory requirements.

More formally, dimensionality reduction is possible whenever the data lie on one manifold (or more) characterized by a lower dimension than what was observed. We call the dimension of this latent, potentially non-linear manifold the *intrinsic dimension* (*id*). Several other definitions of *id* exist in the literature. For example, we can see the *id* as the minimal number of parameters needed to represent all the information contained in the data without significant information loss [Ansuini et al., 2019, Rozza et al., 2011, Bennett, 1969]. Intuitively, the *id* is an indicator of the complexity of the features of a dataset. It is a necessary piece of information to have before attempting to perform any dimensionality reduction, manifold learning, or visualization tasks. Indeed, most dimensionality reduction methods would be worthless without a reliable estimate of the true *id* they need to target: a too-small *id* value can cause needless information loss, while the reverse can lead to an unnecessary waste of time and computational resources [Hino et al., 2017].

Over the past few decades, a vast number of methods for *id* estimation and dimensionality reduction have been developed. The algorithms can be broadly classified into two main categories: projection methods and geometric methods. The former maps the original data to a lower-dimensional space. The projection function can be linear, as in the case of Principal Component Analysis (PCA) [Hotelling, 1933] or nonlinear, as in the case of Locally Linear Embedding [Roweis and Lawrence, 2000], Isomap [Tenenbaum et al., 2000], and the tSNE [Laurens and Geoffrey, 2009]. For more examples, see Jolliffe and Cadima [2016] and the references therein. In consequence, there is a plethora of R packages that implement these types of algorithms: for example RDRToolbox [Bartenhagen, 2020], lle [Kayo, 2006], Rtsne [Krijthe, 2015], and the classic `princomp` function from the default package `stats`.

Geometric methods rely instead on the topology of a dataset, exploiting the properties of the distances between data points. Within this family, we can find fractal methods [Falconer, 2003], graphical methods [Costa and Hero, 2004], methods based on likelihood approaches [Levina and Bickel, 2005], and methods based on nearest neighbors distances [Pettis et al., 1979]. Numerous packages are available: for example, for fractal methods alone there are `fractaldim` [Sevcikova et al., 2014], `nonlinearTseries` [Garcia, 2020], and `tseriesChaos` [Di Narzo, 2019], among others. For a recent review of the methods used for *id* estimation we refer to Campadelli et al. [2015].

Given the abundance of methods in this area, several R developers have also attempted to provide unifying collections of dimensionality reduction and *id* estimation methods. For example, valuable ensemble of methodologies are implemented in the packages `ider` [Hino, 2017], `dimred` and `coRanking` [Kraemer et al., 2018], `dyndimred` [Cannoodt and Saelens, 2020], `IDmining` [Golay and Kanevski, 2017], and `intrinsicDimension` [Johnsson and Lund University, 2019]. Among these proposals, the package `Rdimtools` [You, 2020b] stands out, implementing 150 different algorithms, 17 of which are exclusively dedicated to *id* estimation [You, 2020a].

In this paper, we introduce and discuss the R package `intRinsic`, which is openly available at the Github repository at <https://github.com/Fradenti/intRinsic>. The

package implements the TWO-NN, `Gride`, and `Hidalgo` models, three state-of-the-art `id` estimators recently introduced in [Facco et al. \[2017\]](#), [Denti \[2020\]](#) and [Allegra et al. \[2020\]](#), respectively. All are likelihood-based estimators that rely on the theoretical properties of the distances among the nearest neighbors. The first two models yield an estimate of a global, unique `id` for a dataset and are implemented under both the frequentist and Bayesian paradigms. `Hidalgo`, on the other hand, is a Bayesian mixture model that allows for the estimation of clusters of points characterized by heterogeneous `ids`.

The package contains two sets of functions, organized into high-level and low-level routines. The former set contains R functions intended to be user-friendly and straightforward in their usage. Our goal is to make the package as accessible and intuitive as possible by automating most of the tasks. The low-level set represents the core of the package, and it is not exported. The most computationally-intensive low-level functions are written in C++, exploiting the interface with R provided by the packages `Rcpp` and `RcppArmadillo` [[Eddelbuettel and François, 2011](#), [Eddelbuettel and Sanderson, 2014](#)]. The C++ implementation considerably speeds up time-consuming tasks, like running the Gibbs sampler for the Bayesian mixture model `Hidalgo`. Moreover, `intrinsic` is well integrated with external R packages. For example, all the graphical outputs are produced using `ggplot2` [[Wickham, 2016](#)] or `pheatmap` [[Kolde, 2019](#)] and, where appropriate, simulated Monte Carlo Markov Chains (MCMC) are exported as `coda` [[Plummer et al., 2006](#)] objects. Lastly, we extended the generic method `autoplot` from the `ggplot2` package to create a set of ad-hoc plotting functions that interact with the S3 classes defined in package `intrinsic`.

The article is structured as follows. Section 2 introduces and describes the modeling background, linking each method to its corresponding high-level function. Section 3 presents the functions contained in the package with applications to simulated and real microarray datasets. We show how to obtain, manipulate, and interpret the different outputs. Additionally, we assess the robustness of the methods by monitoring how the results vary when the input parameters change. Finally, Section 4 discusses future extensions to the package.

## 2 The modeling background

Let us consider  $\mathbf{X}$ , a collection of  $n$  data points measured over  $D$  variables. We denote each observation as  $x_i \in \mathbb{R}^D$ . Despite being observed over a  $D$ -dimensional space, we suppose that the points lie entirely on a latent manifold  $\mathcal{M}$  with intrinsic dimension (`id`)  $d \leq D$ . Generally, we expect that  $d \ll D$ : a low-dimensional data-generating mechanism can accurately describe the dataset.

Now, we focus on the single data point  $x_i$ . Starting from this point, one can order the remaining  $n - 1$  observations according to their distance from  $x_i$ . In this way, we obtain a list of nearest neighbors (NNs) of increasing order. Formally, let  $\Delta : \mathbb{R}^D \times \mathbb{R}^D \rightarrow \mathbb{R}^+$  be a generic distance function between data points. We denote with  $x_i^{(l)}$  the  $l$ -th NN of  $x_i$  and with  $r_{i,l} = \Delta(x_i, x_i^{(l)})$  their distance, for  $l = 1, \dots, n - 1$ . Given the sequence of NNs for each data point, we can define the *volume of the hyper-spherical shell enclosed between*

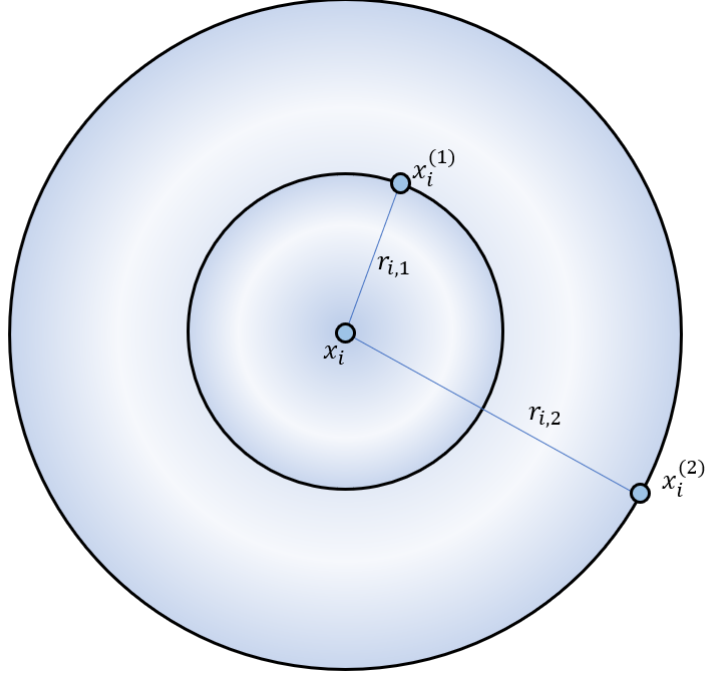


Figure 1: Pictorial representation in  $\mathbb{R}^2$  of the first two NNs of point  $x_i$  and the corresponding distances. In two dimensions, the volume of the hyper-spherical shells  $\nu_{i,1}$  and  $\nu_{i,2}$  is equal to the surfaces of the first circle and the outer ring, respectively.

two successive neighbors of  $x_i$  as

$$\nu_{i,l} = \omega_d \left( r_{i,l}^d - r_{i,l-1}^d \right), \quad \text{for } l = 1, \dots, n-1, \quad \text{and } i = 1, \dots, n, \quad (1)$$

where  $d$  is the dimensionality of the latent manifold in which the points are embedded (the **id**) and  $\omega_d$  is the volume of the  $d$ -dimensional hyper-sphere with unitary radius. For this formula to hold, we need to set  $x_{i,0} \equiv x_i$  and  $r_{i,0} = 0$ . Considering the two-dimensional case for simplicity, we provide a visual representation of the quantities involved in Figure 1 for  $l = 1, 2$ .

From a modeling perspective, we assume the dataset  $\mathbf{X}$  is a realization of a Poisson point process characterized by density function  $\rho(x)$ . [Facco et al. \[2017\]](#) showed that the hyper-spherical shells defined in Equation (1) are the multivariate extension of the well-known *inter-arrival times* [[Kingman, 1992](#)]. Therefore, they proved that under the assumption of homogeneity of the Poisson point process, i.e.  $\rho(x) = \rho \forall x$ , all the  $\nu_{i,l}$ 's are independently drawn from an Exponential distribution with rate equal to the density  $\rho$ :  $\nu_{i,l} \sim \text{Exp}(\rho)$ , for  $l = 1, \dots, n-1$ , and  $i = 1, \dots, n$ . This fundamental result motivates the derivation of the estimators we will introduce in the following sections.



## 2.1 The TWO-NN family of estimators

Building on the distribution of the hyper-spherical shells, [Facco et al. \[2017\]](#) noticed that, if the intensity of the Poisson point process is assumed to be constant on the scale of the second NN, the following distributional result holds:

$$\mu_i = \frac{r_{i,2}}{r_{i,1}} \sim \text{Pareto}(1, d), \quad \mu_i \in (1, +\infty) \quad i = 1, \dots, n. \quad (2)$$

In other words, if the intensity of the Poisson point process that generates the data can be regarded as locally constant (on the scale of the second NN), the ratio of the first two distances from the closest two NNs is Pareto distributed. Recall that the Pareto random variable is characterized by a scale parameter  $a$ , shape parameter  $b$ , and density function  $f_X(x) = ab^a x^{-a-1}$  defined over  $x \in [a, +\infty]$ . Remarkably, Equation (2) states that the ratio  $r_{i,2}/r_{i,1}$  follows a Pareto distribution with scale  $a = 1$  and shape  $b = d$ , i.e. the shape parameter can be interpreted as the `id` of the data. We regard the `id` estimation methods derived from this result as members of the TWO-NN family of estimators. To obtain the vector  $\boldsymbol{\mu} = (\mu_i)_{i=1}^n$ , one can use the `intrinsic` function `generate_mus`. Once the vector  $\boldsymbol{\mu}$  is collected, we can employ different estimators for the `id`.

**Linear Estimator.** [Facco et al. \[2017\]](#) proposed to estimate the `id` via the linearization of the Pareto c.d.f.  $F(\mu_i) = (1 - \mu_i^{-d})$ . The estimate  $\hat{d}_{OLS}$  is obtained as the solution of

$$-\log(1 - \hat{F}(\mu_{(i)})) = d \log(\mu_{(i)}), \quad (3)$$

where  $\hat{F}(\cdot)$  denotes the empirical c.d.f. of the sample and the  $\mu_{(i)}$ 's are the ratios defined in Equation (2) sorted by increasing order. To obtain a more robust estimation, the authors suggested trimming from  $\boldsymbol{\mu}$  a percentage  $\alpha_{TR}$  of the most extreme values. This choice is justified because the extreme ratios often correspond to observations that do not comply with the local homogeneity assumption. This estimator is implemented within the function `linfit_TWONN`.

**Maximum Likelihood Estimator.** In a similar spirit, [Denti \[2020\]](#) took advantage of the distributional results in Equation (2) to derive a simple Maximum Likelihood Estimator (MLE) and corresponding Confidence Interval (CI). Trivially, the (unbiased) MLE for the shape parameter of a Pareto distribution is given by:

$$\hat{d} = \frac{n-1}{\sum_i^n \log(\mu_i)}, \quad (4)$$

while the corresponding CI of level  $(1-\alpha)$  is defined as

$$CI(d, 1-\alpha) = \left[ \frac{\hat{d}}{q_{IG_{n,(n-1)}}^{1-\alpha/2}}, \frac{\hat{d}}{q_{IG_{n,(n-1)}}^{\alpha/2}} \right], \quad (5)$$

where  $q_{IG_{a,b}}^{\alpha/2}$  denotes the quantile of order  $\alpha/2$  of an Inverse-Gamma distribution of shape  $a$  and scale  $b$ . The MLE estimate and CI can be obtained with the function `mle_twonn`.

**Bayesian Estimator.** It is also straightforward to derive an estimator according to a Bayesian perspective. Indeed, one can specify a prior distribution on the shape parameter  $d$ . The most natural prior to choose is a conjugate  $d \sim \text{Gamma}(a, b)$ . It is immediate to derive the posterior distribution for the shape parameter:

$$d|\boldsymbol{\mu} \sim \text{Gamma}\left(a + n, b + \sum_{i=1}^n \log(\mu_i)\right). \quad (6)$$

With the function `bayesfit_twonnn`, one can obtain the principal quantiles of the posterior distribution, collecting point estimates and uncertainty quantification with a credible interval (CrI) of level  $\alpha$ .

## 2.2 The Gride estimator

Denti [2020] also extended the previous theoretical framework by deriving the distribution of the ratio of two generic distances from a point  $x_i$  and two of its NNs of generic order. Let us consider two integers  $n_1 < n_2$  and assume that the density  $\rho$  is approximately locally constant on the scale defined by the distance of the  $n_2$ -th NN, denoted as  $r_{i,n_2}$ . Moreover, we define

$$\dot{\mu}_i = \mu_{i,n_1,n_2} = \frac{r_{i,n_2}}{r_{i,n_1}}. \quad (7)$$

It is possible to derive a closed-form density for the random variable  $\dot{\mu}$ :

$$f_{\mu_{i,n_1,n_2}}(\dot{\mu}) = (n_2 - n_1) \binom{n_2 - 1}{n_1 - 1} \frac{d(\dot{\mu}^d - 1)^{n_2 - n_1 - 1}}{\dot{\mu}^{(n_2 - 1)d + 1}}, \quad \dot{\mu} \in (1, +\infty). \quad (8)$$

Starting from this distribution, they are able to propose the generalized ratio intrinsic dimension estimator (**Gride**) family. Unfortunately, closed-form representation for the MLE and CI are not available. We need to resort to numerical optimization and parametric bootstrapping within the frequentist framework and MCMC simulation within the Bayesian setting. To do so, we can use the functions `mle_gride`, `bootstrap_gride`, and `bayesfit_gride`.

## 2.3 The Hidalgo model

All the estimators we described in the previous sections implicitly assume that the `id` of a dataset is unique. However, considering a single value for the `id` can often be limiting, especially when the data present complex dependence structures among variables. To extend the previous modeling framework, one can imagine that the data points are divided into clusters, each of them lying on a latent manifold with its specific `id`. Allegra et al. (2020) employed this heterogeneous `id` estimation approach in their model: the heterogeneous `id` algorithm (**Hidalgo**). The authors assumed that the density function of the generating point process is in fact a mixture of  $K$  distributions defined on  $K$  different latent manifolds, expressed as  $\rho(\mathbf{x}) = \sum_{k=1}^K \pi_k \rho_k(\mathbf{x})$ , where  $\boldsymbol{\pi} = (\pi_1, \dots, \pi_K)$  is the vector of mixture

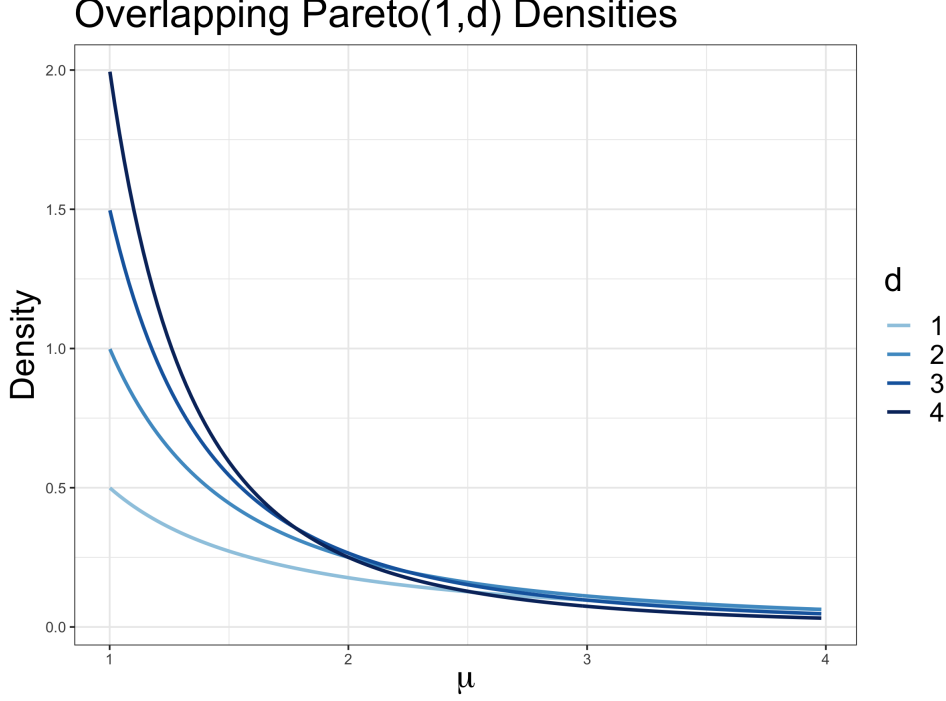


Figure 2: Density functions of  $Pareto(1, d)$  distribution for different values of the shape parameter  $d$ .

weights. This assumption induces a mixture of Pareto distributions as the distribution of the ratios  $\mu_i$ 's:

$$\mu_i | \mathbf{d}, \boldsymbol{\pi} = \sum_{k=1}^K \pi_k d_k \mu_i^{-(d_k+1)}, \quad (9)$$

where  $\mathbf{d} = (d_1, \dots, d_K)$  is the vector of different ids and  $\boldsymbol{\pi}$  is the vector containing the  $K$  mixture weights. Allegra et al. [2020] adopted a Bayesian perspective, specifying independent Gamma priors for each element of  $\mathbf{d}$ :  $d_k \sim \text{Gamma}(a_d, b_d)$ , and a Dirichlet prior for the mixture weights  $\boldsymbol{\pi} \sim \text{Dirichlet}(\alpha_1, \dots, \alpha_K)$ .

Unfortunately, a model-based clustering approach such as the one presented in Equation (9) is ineffective at modeling the data. The problem lies in the fact that the different Pareto kernel densities constituting the mixture components are extremely similar and overlapping. Therefore, Pareto densities with varying shape parameters can fit the same data points equally well, compromising the clustering. Even when considering very diverse shape parameters, the right tails of the different Pareto distributions overlap to a great extent. This issue is evident in Figure 2, where we illustrate different examples of  $Pareto(1, d)$  densities. Thus, the distributional similarity jeopardizes the cluster assignments of the data points and the consequent ids estimation.

To address this problem, Allegra et al. [2020] introduced a local homogeneity assumption, which postulates that points close to each other are more likely to be part of the

same latent manifold. To incorporate this, the authors added an extra penalizing term in the likelihood. We now summarize their approach.

First, they introduced the latent membership labels  $\mathbf{z} = (z_1, \dots, z_n)$  to assign each observation to a cluster, where  $z_i = k$  means that the  $i$ -th observation was assigned to the  $k$ -th mixture component. Then, they defined the binary adjacency matrix  $\mathcal{N}^{(q)}$ , whose entries are  $\mathcal{N}_{ij}^{(q)} = 1$  if the point  $x_j$  is among the  $q$  NNs of  $x_i$  and 0 otherwise. Finally, they assumed the following probabilities:  $\mathbb{P}[\mathcal{N}_{ij}^{(q)} = 1 | z_i = z_j] = \zeta_1$ , with  $\zeta_1 > 0.5$  and  $\mathbb{P}[\mathcal{N}_{ij}^{(q)} = 1 | z_i \neq z_j] = \zeta_0$ , with  $\zeta_0 < 0.5$ . These probabilities are incorporated in the following distributional constraints for the data point  $x_i$ :  $\pi(\mathcal{N}_i^{(q)} | \mathbf{z}) = \prod_{j=1}^n \zeta_0^{\mathbb{1}_{z_i \neq z_j}} \zeta_1^{\mathbb{1}_{z_i = z_j}} / \mathcal{Z}_i$ , where  $\mathcal{Z}_i$  is the normalizing constant and  $\mathbb{1}_A$  is the indicator function, equal to 1 when the event  $A$  is true, 0 otherwise. A more technical discussion of this model extension and the validity of the underlying hypothesis can be found in the Supplementary Material of [Allegre et al. \[2020\]](#). For simplicity, we assume  $\zeta_0 = \zeta$  and  $\zeta_1 = 1 - \zeta$ . The model becomes

$$\mathcal{L}(\mu_i, \mathcal{N}^{(q)} | \mathbf{d}, \mathbf{z}, \zeta) = d_{z_i} \mu_i^{-(d_{z_i}+1)} \times \prod_{i=1}^n \frac{\zeta^{\mathbb{1}_{z_i \neq z_j}} (1 - \zeta)^{\mathbb{1}_{z_i = z_j}}}{\mathcal{Z}_i}, \quad z_i | \boldsymbol{\pi} \sim \text{Cat}_K(\boldsymbol{\pi}), \quad (10)$$

where  $\text{Cat}_K$  denotes a Categorical distribution over  $\{1, \dots, K\}$ . A closed-form for the posterior distribution is not available, so we rely on MCMC techniques to simulate a posterior sample. The function `Hidalgo` implements the Bayesian mixture model under the conjugate prior and two other alternative distributions. When the nominal dimension  $D$  is low, the unbounded support of a Gamma prior may provide unrealistic results, where the posterior distribution assigns positive density to the interval  $(D, +\infty)$ . [Santos-Fernandez et al. \[2020\]](#) proposed to employ a more informative prior for  $\mathbf{d}$ :

$$\pi(d_k) = \hat{\rho} \cdot d_k^{a-1} \exp^{-bd_k} \frac{\mathbb{1}_{(0,D)}}{\mathcal{C}_{a,b,D}} + (1 - \hat{\rho}) \cdot \delta_D(d_k) \quad \forall k, \quad (11)$$

where they denoted the normalizing constant of a  $\text{Gamma}(a, b)$  truncated over  $(0, D]$  with  $\mathcal{C}_{a,b,D}$ . That is, the prior distribution for  $d_k$  is a mixture between a truncated Gamma distribution over  $(0, D]$  and a point mass located at  $D$ . The parameter  $\rho$  denotes the mixing proportion. When  $\rho = 1$ , the distribution in (11) reduces to a simple truncated Gamma. Both approaches are implemented in `intRinsic`.

The steps of the Gibbs sampler are the following:

1. Sample the mixture weights according to

$$\boldsymbol{\pi} | \dots \sim \text{Dirichlet} \left( \alpha_1 + \sum_{i=1}^n \mathbb{1}_{z_i=1}, \dots, \alpha_K + \sum_{i=1}^n \mathbb{1}_{z_i=K} \right)$$

2. Let  $\mathbf{z}_{-i}$  denote the vector  $\mathbf{z}$  without its  $i$ -th element. Sample the cluster indicators  $z_i$  according to:

$$\mathbb{P}(z_i = k | \mathbf{z}_{-i}, \dots) \propto \pi_{z_i} f(\mu_i, \mathcal{N}_i^{(q)} | z_1, \dots, z_{i-1}, k, z_{i+1}, \dots, z_n, \mathbf{d})$$

We emphasize that, given the new likelihood we are considering, the cluster labels are no longer independent given all the other parameters. Let us define

$$\mathbf{z}_i^k = (z_1, \dots, z_{i-1}, k, z_{i+1}, \dots, z_n).$$

Then, let  $N_{z_i}(\mathbf{z}_{-i})$  be the number of elements in the  $(n-1)$ -dimensional vector  $\mathbf{z}_{-i}$  that are assigned to the same manifold (mixture component) as  $z_i$ . Moreover, let  $m_i^{in} = \sum_l \mathcal{N}_{li}^{(q)} \mathbb{1}_{z_l=z_i}$  be the number of points sampled from the same manifold of the  $i$ -th observation that have  $x_i$  as neighbor, and let  $n_i^{in}(\mathbf{z}) = \sum_l \mathcal{N}_{il}^{(q)} \mathbb{1}_{z_l=z_i} \leq q$  be the number of neighbors of  $x_i$  sampled from the same manifold. Then, we can simplify the previous formula, obtaining the following full conditional:

$$\begin{aligned} \mathbb{P}(z_i = k | \mathbf{z}_{-i}, \dots) &\propto \frac{\pi_k d_k \mu_i^{-(d_k+1)}}{\mathcal{Z}(\zeta, N_{z_i=k}(\mathbf{z}_{-i}) + 1)} \times \left( \frac{\zeta}{1-\zeta} \right)^{n_i^{in}(\mathbf{z}_i^k) + m_i^{in}(\mathbf{z}_i^k)} \\ &\times \left( \frac{\mathcal{Z}(\zeta, N_{z_i=k}(\mathbf{z}_{-i}))}{\mathcal{Z}(\zeta, N_{z_i=k}(\mathbf{z}_{-i}) + 1)} \right)^{N_{z_i=k}(\mathbf{z}_{-i})}. \end{aligned} \quad (12)$$

See [Facco and Laio \[2017\]](#) for a detailed derivation of this result.

3. The posterior distribution for  $\mathbf{d}$  depends on the prior specification we adopt:
  - a) If we assume a conjugate Gamma prior, we obtain

$$d_k | \dots \sim \text{Gamma} \left( a_0 + n_k, b_0 + \sum_{i:z_i=k} \log \mu_i \right),$$

where  $n_k = \sum_{i=1}^n \mathbb{1}_{z_i=k}$  is the number of observations assigned to the  $k$ -th group;

- b) If  $G_0$  is assumed to be a truncated Gamma distribution on  $(0, D)$ , then

$$d_k | \dots \sim \text{Gamma} \left( a_0 + n_k, b_0 + \sum_{i:z_i=k} \log \mu_i \right) \mathbb{1}(\cdot)_{(0,D)};$$

- c) Finally, let us define  $a^* = a_0 + n_k$  and  $b^* = b_0 + \sum_{i:z_i=k} \log \mu_i$ , if  $G_0$  is assumed to be a truncated Gamma with point mass at  $D$  we obtain

$$d_k | \dots \sim \frac{\hat{\rho}_1^*}{\hat{\rho}_1^* + \hat{\rho}_0^*} \text{Gamma}(a^*, b^*) \mathbb{1}(\cdot)_{(0,D)} + \frac{\hat{\rho}_0^*}{\hat{\rho}_1^* + \hat{\rho}_0^*} \delta_D(d_k),$$

where  $\hat{\rho}_1^* = \hat{\rho} \frac{C_{a^*, b^*, D}}{C_{a, b, D}}$  and  $\hat{\rho}_0^* = (1 - \hat{\rho}) D^{n_k} \exp^{-D \sum_{i:z_i=k} \log \mu_i}$ .

The algorithm for the Gibbs sampler concludes our brief introduction of the novel `id` estimators implemented in `intRinsic`. Table 1 summarizes the main characteristics of the three approaches we discussed.

Model	Frequentist	Bayesian	NN Ratio Scale	id
TWO-NN	✓	✓	Second to First	Homogeneous
GrIde	✓	✓	General	Homogeneous
Hidalgo	✗	✓	Second to First	Heterogeneous

Table 1: Summary of the estimators included in the `intRinsic` package.

### 3 Examples using `intRinsic`

This section illustrates and discusses the main routines of the `intRinsic` package. We apply our `id` estimation techniques to four datasets. The first three datasets are simulated. That way, we can compare the results of the different experiments with the ground truth. Then, our methods are employed to estimate the `ids` present in the `Alon` microarray table, contained in the R package `HiDimDa` [Silva, 2015]. To start with the illustration, we first load our package by running:

```
R> library(intRinsic)
```

In the following, we will indicate the number of observations and the observed nominal dimension with `n` and `D`, respectively. The `id` value is denoted with `d`. Let us also represent with  $\mathcal{N}_k(m, \Sigma)$  a multivariate Normal distribution of dimension  $k$ , mean  $m$ , and covariance matrix  $\Sigma$ . Moreover, let  $\mathcal{T}_{g,k}$  represent a multivariate Student's t-distribution with  $g$  degrees of freedom in  $k$  dimensions. Finally, we denote  $\mathbb{I}_k$  as an identity matrix of dimension  $k$  and  $\mathbb{1}_A$  as the indicator function equal to 1 when event  $A$  is true.

#### 3.1 Simulated Datasets

For the first part of the illustration, we consider three different simulated datasets:  $\mathcal{D}_1$ ,  $\mathcal{D}_2$ , and  $\mathcal{D}_3$ . The first one is obtained via the classical Swissroll transformation  $\mathcal{S} : \mathbb{R}^2 \rightarrow \mathbb{R}^3$  defined as  $\mathcal{S}(x, y) = (x \cos(x), y, x \sin(x))$ . Each pair of points  $(x, y)$  mapped with the Swissroll transformation is sampled from two independent Uniform distributions on  $(0, 10)$ . To simulate such a dataset, use the function `Swissroll_maker` specified with the number of observations `N` as the input parameter.  $\mathcal{D}_2$  contains a cloud of points sampled from  $\mathcal{T}_{8,5}$  embedded in an eight-dimensional space  $\mathbb{R}^8$ . Lastly, the dataset  $\mathcal{D}_3$  is the collection of data points generated from three different random variables,  $X_1, X_2$ , and  $X_3$ , embedded in a five-dimensional Euclidean space. In particular, the three random variables are distributed as

$$X_1 = 3X_0, \quad X_0 \sim \mathcal{N}_1(0, 1); \quad X_2 \sim \mathcal{N}_3(0, \mathbb{I}_3); \quad X_3 \sim \mathcal{N}_5(5, \mathbb{I}_5).$$

One can generate the exact replica of the three simulated datasets used in this paper by running the following code:

```
R> set.seed(123456)
R> Swissroll <- as_tibble(Swissroll_maker(N = 1000))
```

Dataset	Name	n	D	d
$\mathcal{D}_1$	Swissroll	1000	3	2
$\mathcal{D}_2$	Student_T	500	8	5
$\mathcal{D}_3$	GaussMix	1500	5	??

Table 2: Summary of the dimensionality characteristics of the three simulated datasets.

```
R> Student_T <- replicate(5, rt(500, 8))
R> Student_T <- as_tibble(cbind(Student_T, 0, 0, 0))
R> v1 <- rnorm(500, -5, sd = 2)
R> v1 <- cbind(x = v1, y = 3 * v1, 0, 0, 0)
R> v2 <- cbind(replicate(3, rnorm(500)), 0, 0)
R> v3 <- replicate(5, rnorm(500, 5))
R> GaussMix <- as_tibble(rbind(v1, v2, v3))
R> GaussMix <- GaussMix %>%
+   mutate(Mix_comp = rep(c("A", "B", "C"), rep(500, 3)))
```

Table 2 summarizes the sample sizes along with the nominal and intrinsic dimensions that characterize the three datasets. To visualize the data, we can use the `PairPlot` function from the `WVPlots` package.

```
R> WVPlots::PairPlot(d = Swissroll, meas_vars = c("x", "y", "z"),
+   title = "Swiss Roll dataset",
+   point_color = "royalblue", alpha = .5)
```

These scatterplots can be useful as an exploratory tool to spot any clear dependence across the columns of a dataset. The plot provides us with a qualitative idea about the value of the `id` that should be expected. For example, applying the function `PairPlot` to the `Swissroll` dataset we obtain Figure 3. From the different panels, it is evident that two of the three coordinates are free, and we can recover the last coordinate as a function of the others. Therefore, the `id` of  $\mathcal{D}_1$  is equal to 2. From the description of the data simulation, it is also evident that the `id`=5 for the second dataset  $\mathcal{D}_2$ . However, it is not as simple to figure out the value of the ground truth `id` for  $\mathcal{D}_3$ , given the heterogeneity of its data generating mechanism.

### 3.2 Ratios of nearest neighbors distances

The ratios between distances of NNs constitute the fundamental quantities on which the theoretical development presented in Section 2 is based. We can compute the ratios  $\mu_i$  defined in Equation (2) with the function `generate_mus`. The function takes the following arguments:

- **X**: a dataset of dimension  $n \times D$  of which we want to compute the ratios  $\mu_i$ 's;

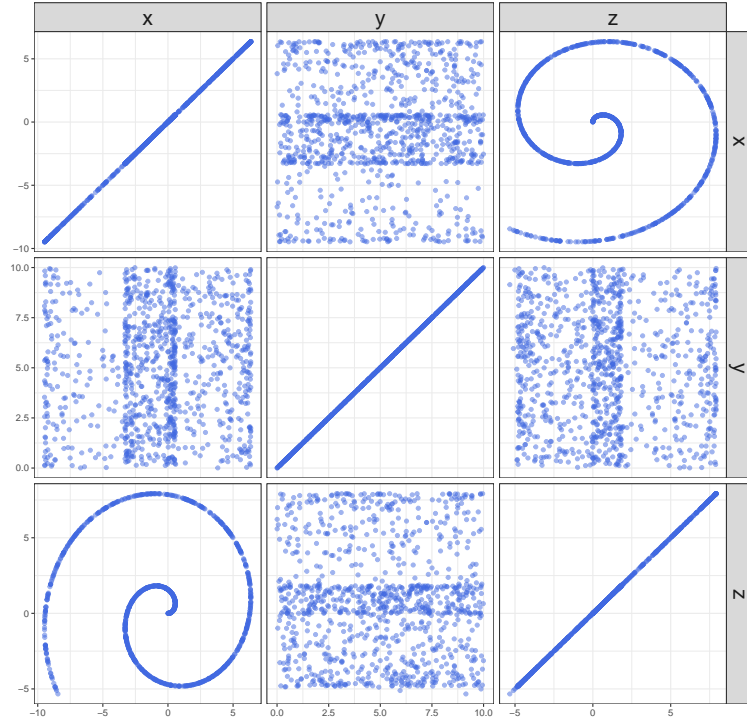


Figure 3: Scatterplot of the three variables in the **Swissroll** dataset obtained with the function **PairPlot**. The dependence among the coordinates  $x$  and  $z$  is evident.

- **dupl\_remove**: logical, if **TRUE** the function automatically detects and removes duplicates in the sample;
- **DM**: a  $n \times n$  user-provided distance matrix. If **NULL**, the function automatically detects the NNs in terms of Euclidean distance.

The output of the function is the vector of ratios  $\boldsymbol{\mu} = \{\mu_i\}_{i=1}^n$ . For example, we can write:

```
R> mus_Swiss      <- generate_mus(X = Swissroll)
R> mus_Students  <- generate_mus(X = Student_T)
R> mus_GaussMix  <- generate_mus(X = GaussMix %>% select(-Mix_comp))
```

The histograms of the three datasets' estimated ratios are reported in Figure 4. All of the histograms present the right-skewed shape typical of Pareto distribution. If the distance matrix **DM** is not specified, **generate\_mus** relies on the function **get.knn** from the package **FNN** [Beygelzimer et al., 2019], which implements fast NN-search algorithms. Recall that the model is based on the assumption that a Poisson point process is the generating mechanism of the dataset. Ergo, the model cannot handle situations where ties among data points are present. From a more practical point of view, if  $\exists i \neq j$  such that



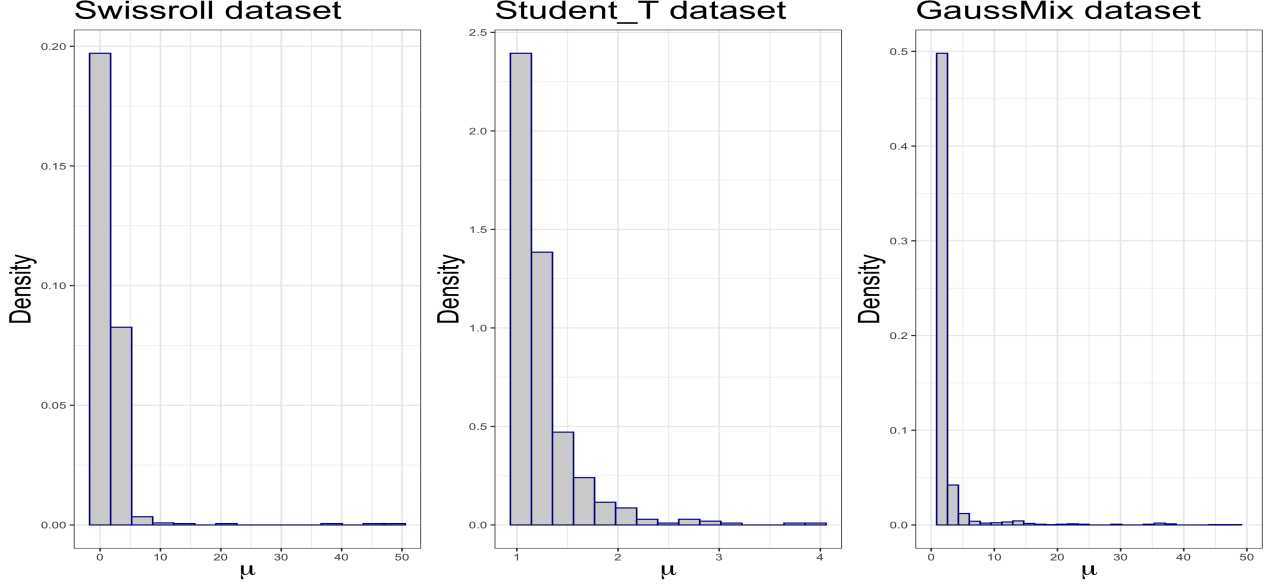


Figure 4: Histograms of the ratios  $\mu = \{\mu_i\}_{i=1}^n$  for datasets  $\mathcal{D}_1$ ,  $\mathcal{D}_2$ , and  $\mathcal{D}_3$ . The shape of the histograms suggests that a Pareto distribution could be a good fit.

$x_i = x_j$ , the computation of  $\mu_i$  would be infeasible, since  $r_{i,1} = 0$ . We devised the function `generate_mus` to automatically detect and remove duplicates in a dataset if the argument `dupl_remove` is set to `TRUE`. In case `dupl_remove` is set to `FALSE`, the function stops and locates the problematic observations. Let us showcase this behavior with a simple example:

```
R> DummyData <- rbind(c(1, 2, 3), c(1, 4, 3), c(1, 2, 3),
+                     c(1, 4, 3), c(1, 4, 3), c(1, 4, 3), c(1, 1, 1))
R> generate_mus(X = DummyData, dupl_remove = F, DM = NULL)
```

```
Duplicates are present in the dataset.
I cannot proceed!
The problematic indexes are:
[1] 3 4 5 6
```

This function is the core of the higher-level, intuitive routines we use to estimate the `id`. In the following subsections, we show how to use the `TWO-NN` and `GrIde` models to obtain a unique, homogeneous `id` estimate for each dataset.

### 3.3 TWO-NN: homogeneous intrinsic dimension estimator

Let us start with the `TWO-NN` model presented in Section 2.1. In alignment with recent developments in the literature, we propose three methods to carry out inference on the `id` value: the linear estimator, the MLE, and Bayesian approach.

	Swissroll	Swissroll	Student_T	Student_T
	Not trimmed	1% trimmed	Not trimmed	1% trimmed
R object	lin11	lin12	lin21	lin22
Lower Bound	1.9524	2.2333	4.7476	5.2052
Estimate	1.9669	2.2456	4.7753	5.2263
Upper Bound	1.9814	2.2580	4.8031	5.2474

Table 3: Point estimate and relative confidence intervals for the `id` values retrieved with the linear estimator. The estimates change when removing the 1% of most extreme ratios.

### 3.3.1 Linear Estimator

The function `linfit_twonnn` implements the regression stated in Equation (3) and needs the following objects as input: the dataset `X` or the distance matrix `DM` (see the previous function's arguments specification for more details), and

- `trimmed`: logical, if `TRUE` a percentage of the most extreme observations is discarded to help improve the estimation;
- `alpha_trimmed`: the percentage of extreme observations to discard before the linear estimation is performed.

The function returns a list of class `lnf_twonnn` as output. The first element is the vector `Estimates`, containing the `id` point estimate and the relative 95% confidence interval. The second element, `Lin_mod` is the output of the linear regression performed within the function `linfit_twonnn`.

We apply this estimator to  $\mathcal{D}_1$  and  $\mathcal{D}_2$ . We compare the estimates with and without trimming, creating four R objects. Table 3 displays the estimates obtained by running the following code:

```
R> lin11 <- linfit_twonnn(X = Swissroll, trimmed = F, alpha_trimmed = 0)
R> lin12 <- linfit_twonnn(X = Swissroll, trimmed = T, alpha_trimmed = 0.01)
R> lin21 <- linfit_twonnn(X = Student_T, trimmed = F, alpha_trimmed = 0)
R> lin22 <- linfit_twonnn(X = Student_T, trimmed = T, alpha_trimmed = 0.01)
```

We can also plot the data and the relative regression line using the generic function `autoplot`. Examples of plots obtained from this experiment are shown in Figure 5. The slope of the regression lines corresponds to the linear fit `id` estimates.

```
R> autoplot(lin12) + ggtitle("Swissroll - 0.1% trimmed")
R> autoplot(lin22) + ggtitle("Student_T - 0.1% trimmed")
```

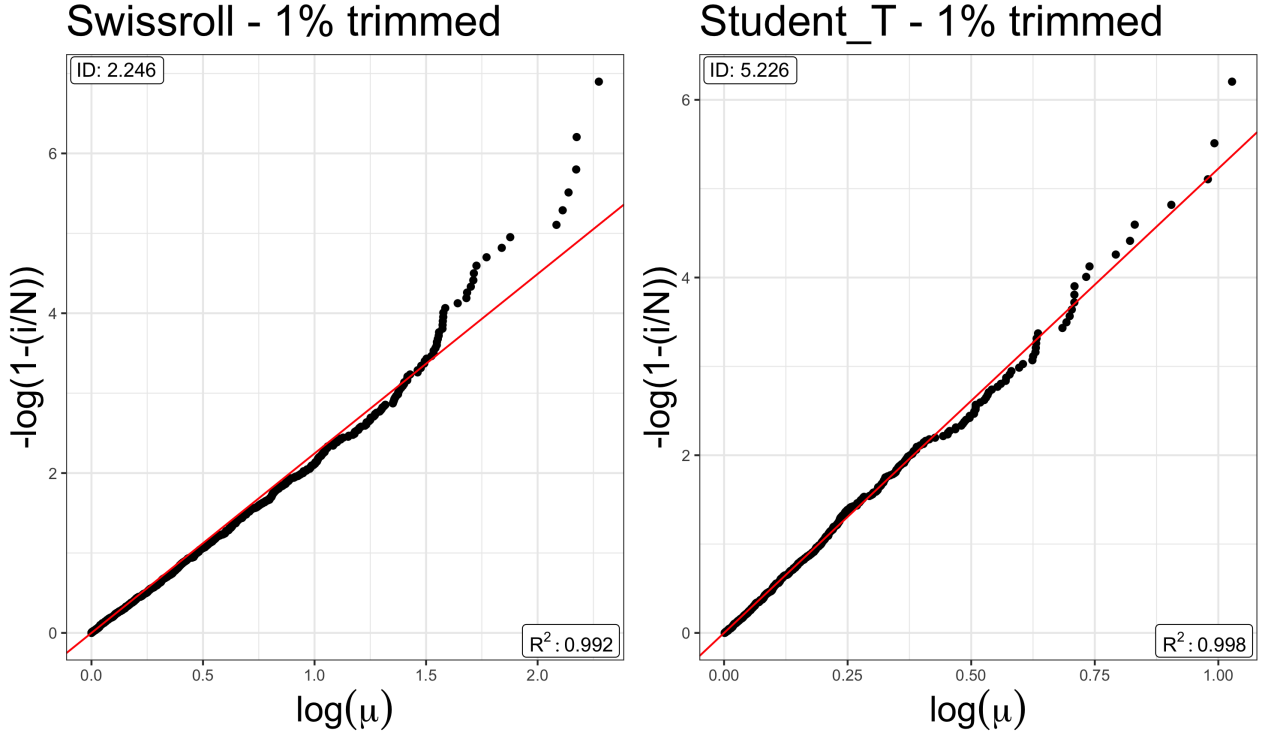


Figure 5: Linear regression fitted to the set of points  $-\log(1 - \hat{F}(\mu_i)) = d \log(\mu_i)$  for the **Swissroll** dataset (left panel) and **Student.T** dataset (right panel).

### 3.3.2 Maximum Likelihood Estimator

A second way to obtain an `id` estimate, along with its confidence interval, is via MLE. The formulas implemented are presented in Equations (4) and (5). We can obtain the ML estimate with the `mle_twonm` function, which takes six arguments. Four arguments are identical to those which we have already discussed: `X`, `trimmed`, `alpha_trimmed`, and `DM`. The last two arguments are:

- `conf_lev`: the confidence level specified to compute the confidence interval for the MLE. The default is 0.95;
- `unbiased`: logical, if `TRUE` the point estimate according to the unbiased estimator (where the numerator is  $n - 1$ , as in Equation (4)) is computed.

We present an example with two different distance matrices: one computed using the Euclidean distance, the other using the Manhattan distance. To obtain the distance matrices for  $\mathcal{D}_1$  and  $\mathcal{D}_2$ , we write:

```
R> dist_Eucl_Sw <- as.matrix(stats::dist(Swissroll))
R> dist_Manh_Sw <- as.matrix(stats::dist(Swissroll, method = "manhattan"))
R> dist_Eucl_St <- as.matrix(stats::dist(Student_T))
```

```
R> dist_Manh_St <- as.matrix(stats::dist(Student_T, method = "manhattan"))
```

We can now run the function `mle_twonn` to obtain `id` estimates under different scenarios. Specifically, we first run `mle_twonn` specifying only the dataset `X` (`m11`, `m14`). The function will automatically detect the NNs using Euclidean distances. We also supply the Euclidean distance matrix (`m12`), which is an equivalent result to `m11` and since we set `DM=NULL`. Lastly, we supply the Manhattan distance matrix (`m13`, `m15`). Other distance matrices can be employed as well. We also show how the bounds of the CIs change by varying the confidence levels. The results are summarized in Table 4. The type of distance can lead to differences in the results. However, in this case, the estimators agree with each other, obtaining values that are close to the ground truth.

```
R> m11_Sw <- mle_twonn(X = Swissroll)
R> m12_Sw <- mle_twonn(X = Swissroll, DM = dist_Eucl_Sw)
R> m13_Sw <- mle_twonn(X = Swissroll, DM = dist_Manh_Sw)
R> m14_Sw <- mle_twonn(X = Swissroll, conf_lev = .99)
R> m15_Sw <- mle_twonn(X = Swissroll, DM = dist_Manh_Sw, conf_lev = .90)
R> m11_St <- mle_twonn(X = Student_T)
R> m12_St <- mle_twonn(X = Student_T, DM = dist_Eucl_St)
R> m13_St <- mle_twonn(X = Student_T, DM = dist_Manh_St)
R> m14_St <- mle_twonn(X = Student_T, conf_lev = .99)
R> m15_St <- mle_twonn(X = Student_T, DM = dist_Manh_St, conf_lev = .90)
```

Dataset	R object	Distance	$\alpha$	Lower Bound	Estimate	Upper Bound
Swissroll	m11_Sw	Eucl	0.95	1.9320	2.0555	2.1870
	m12_Sw	Eucl	0.95	1.9320	2.0555	2.1870
	m13_Sw	Manh	0.95	1.9371	2.0609	2.1928
	m14_Sw	Eucl	0.99	1.8938	2.0555	2.2290
	m15_Sw	Manh	0.90	1.9568	2.0609	2.1714
Student_T	m11_St	Eucl	0.95	4.5402	4.9561	5.4106
	m12_St	Eucl	0.95	4.5402	4.9561	5.4106
	m13_St	Manh	0.95	4.7939	5.2330	5.7129
	m14_St	Eucl	0.99	4.4126	4.9561	5.5567
	m15_St	Manh	0.90	4.8638	5.2330	5.6350

Table 4: MLE obtained from the TWO-NN model. Different distance functions and confidence level specifications are adopted.

### 3.3.3 Bayesian Estimation

The third option for `id` estimation is to adopt a Bayesian perspective and specify a prior distribution for the parameter  $d$ . To obtain the Bayesian estimates in this way, we can use

	Vague	Vague	Informative	Informative
R object	bay1	bay2	bay3	bay4
CrI level	$\alpha = 0.95$	$\alpha = 0.99$	$\alpha = 0.95$	$\alpha = 0.99$
Lower Bound	1.9319	1.8937	1.9299	1.8918
Mean	2.0575	2.0575	2.0553	2.0553
Median	2.0568	2.0568	2.0546	2.0546
Mode	2.0554	2.0554	2.0532	2.0532
Upper Bound	2.1869	2.2289	2.1846	2.2265

Table 5: Posterior estimates under the Bayesian specification according to different prior specifications and levels  $\alpha$  of the credible interval.

the function `bayesfit_twonnn`. Along with `X`, `trimmed`, `alpha_trimmed`, and `DM`, we also need to specify:

- `a_d` and `b_d`: shape and rate parameter for the Gamma prior distribution on  $d$ . A vague specification is adopted as a default with `a_d=0.001` and `b_d=0.001`;
- `alpha`: the probability contained in the credible interval computed on the posterior distribution.

In the following, four examples showcase the usage of this function on the `Swissroll` dataset. We compute the estimates under the default specification (`bay1`) with different credible interval levels (`bay2`) and prior specifications (`bay3`), as well as with a combination of the previous settings (`bay4`). The estimates are reported in Table 5.

```
R> bay1 <- bayesfit_twonnn(X = Swissroll)
R> bay2 <- bayesfit_twonnn(X = Swissroll, alpha = 0.99)
R> bay3 <- bayesfit_twonnn(X = Swissroll, a_d = 1, b_d = 1)
R> bay4 <- bayesfit_twonnn(X = Swissroll, a_d = 1, b_d = 1, alpha = .99)
```

We can plot the posterior distribution, as reported in Figure 6, using `autoplot`. When plotting an object returned from `bayesfit_twonnn`, we can also specify the following parameters:

- `plot_low` and `plot_upp`: lower and upper extremes of the support on which the posterior is evaluated.
- `by`: increment of the sequence going from `plot_low` to `plot_upp` that defines the support.

We compare the default vague prior specification with a strongly informative one by writing:

```
R> b1 <- bayesfit_twonnn(X = Swissroll)
R> b2 <- bayesfit_twonnn(X = Swissroll, a_d = 200, b_d = 100)
R> autoplot(b1, plot_low = 1.5, plot_upp = 2.5, by = .01) +
```

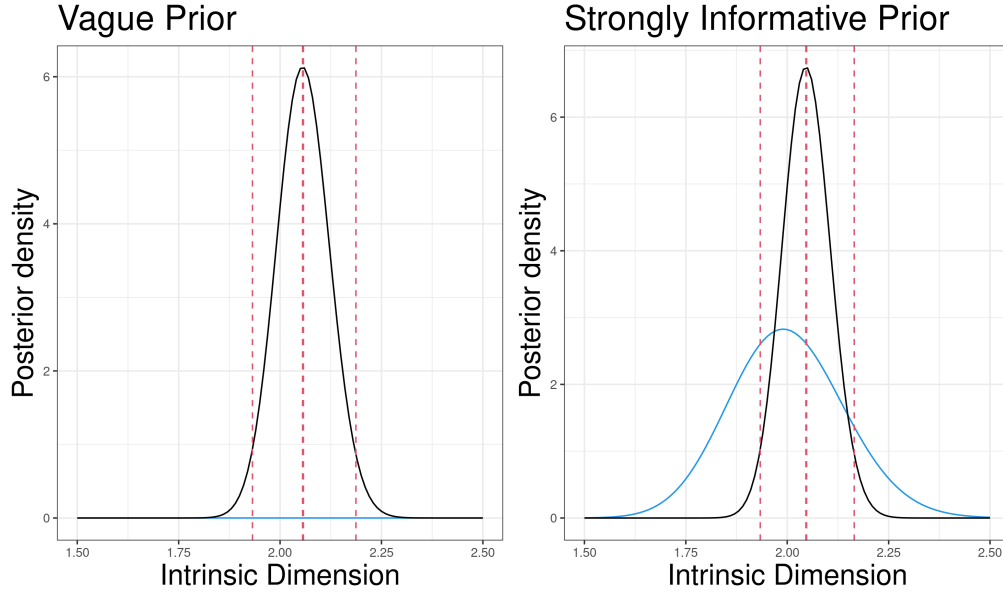


Figure 6: **Swissroll** dataset. Graphical representation of the posterior distribution (black line), prior distribution (blue line), and main quantiles and average (vertical dotted red lines) under vague (left panel) and informative (right panel) prior specifications.

```
+           ggtitle("Vague Prior")
R> autoplot(b2, plot_low = 1.5, plot_upp = 2.5, by = .01) +
+           ggtitle("Strongly Informative Prior")
```

The posterior distribution is depicted in black, the prior in blue, and the dashed vertical red lines represent the estimates.

### 3.4 Grid: intrinsic dimension estimation based on generic ratios of NN distances

Another estimator for the `id` is **Grid**, the TWO-NN generalization proposed in [Denti \[2020\]](#). This estimator is based on the distributional properties of the generic ratios between distances of NNs. Paralleling the structure of core and high-level functions for the TWO-NN model, we start by presenting `generate_mudots`, which computes the ratios as specified in Equation (7). The function `generate_mudots` takes as inputs the dataset `X`, `dupl_remove`, `DM`, and:

- `n1`: integer, the order of the closest NN;
- `n2`: integer, the order of the furthest NN.

It is important to specify the orders of the two NNs `n1` and `n2` where `n1 < n2`. We can use this function in the following way:

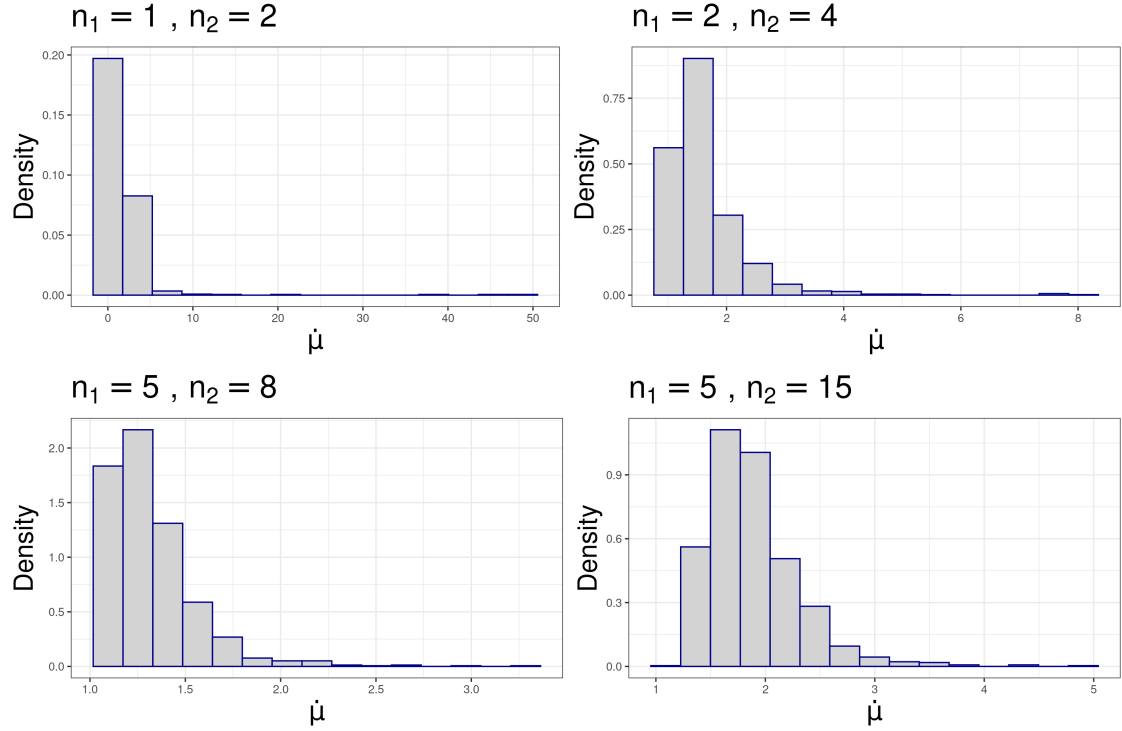


Figure 7: **Swissroll** dataset. Histograms of the generalized ratios  $\dot{\mu} = \{\mu_{i,n_1,n_2}\}_{i=1}^n$  for different values of the NN orders  $n_1$  and  $n_2$ .

```
R> mud1 <- generate_mudots(X = Swissroll, n1 = 1, n2 = 2)
R> mud2 <- generate_mudots(X = Swissroll, n1 = 2, n2 = 4)
R> mud3 <- generate_mudots(X = Swissroll, n1 = 5, n2 = 8)
R> mud4 <- generate_mudots(X = Swissroll, n1 = 5, n2 = 15)
```

From this chunk of code we obtain as output the vectors  $\dot{\mu} = \{\mu_{i,n_1,n_2}\}_{i=1}^n$ . We plot the histograms of the computed vectors in Figure 7. The shape of the distributions varies according to the different ratios of NN order specifications.

As discussed in Section 2.2, the MLE for  $d$  has no closed-form expression given the distribution of  $\dot{\mu}$  in Equation (8). Therefore, we rely on numerical methods to carry out the estimations. The package **intrinsic** implements both a frequentist MLE estimator and a Bayesian estimator. In the former framework, we provide uncertainty quantification via bootstrap sample. For the latter, a Gamma prior for  $d$  is adopted. We simulate the posterior distribution via the Metropolis-Hastings algorithm, with  $\mathcal{N}_1(0, \sigma^2)$  as the proposal distribution over  $\log(d)$ .

### 3.4.1 Maximum Likelihood Estimation

The MLE can be computed with the `mle_gride` function, which has the same input arguments as `generate_mudots`. Here, we report some examples specifying different NN orders and confidence levels. The code to obtain the results for the `Swissroll` dataset is:

```
R> sw11 <- mle_gride(Swissroll, n1 = 1, n2 = 2)
R> sw21 <- mle_gride(Swissroll, n1 = 2, n2 = 4)
R> sw31 <- mle_gride(Swissroll, n1 = 5, n2 = 8)
R> sw41 <- mle_gride(Swissroll, n1 = 5, n2 = 15)
R> sw12 <- mle_gride(Swissroll, n1 = 1, n2 = 2, conf_lev = .99)
R> sw22 <- mle_gride(Swissroll, n1 = 2, n2 = 4, conf_lev = .99)
R> sw32 <- mle_gride(Swissroll, n1 = 5, n2 = 8, conf_lev = .99)
R> sw42 <- mle_gride(Swissroll, n1 = 5, n2 = 15, conf_lev = .99)
```

Similarly, for the `Student.T` dataset we have:

```
R> st11 <- mle_gride(Student_T, n1 = 1, n2 = 2)
R> st21 <- mle_gride(Student_T, n1 = 2, n2 = 4)
R> st31 <- mle_gride(Student_T, n1 = 5, n2 = 8)
R> st41 <- mle_gride(Student_T, n1 = 5, n2 = 15)
R> st12 <- mle_gride(Student_T, n1 = 1, n2 = 2, conf_lev = .99)
R> st22 <- mle_gride(Student_T, n1 = 2, n2 = 4, conf_lev = .99)
R> st32 <- mle_gride(Student_T, n1 = 5, n2 = 8, conf_lev = .99)
R> st42 <- mle_gride(Student_T, n1 = 5, n2 = 15, conf_lev = .99)
```

The results are reported in Table 6. The main function `mle_gride` calls the function `bootstrap_gride` to perform parametric bootstrap to provide an approximate confidence interval for the parameter  $d$ . The function `bootstrap_gride` takes as arguments the objects `X`, `n1`, `n2`, all previously discussed, and `nsim`, the number of bootstrap samples that we want to generate. The default is set to 2000. For example, we can collect a bootstrap sample with:

```
R> bootsam <- bootstrap_gride(X = Swissroll, n1 = 2, n2 = 4, nsim = 2000)
```

The left panel of Figure 8 shows the density plot of the bootstrap sample generated with the previous line of code.

### 3.4.2 Bayesian Estimator

Under the Bayesian paradigm, we can sample from the posterior distribution  $\pi(d|\hat{\mu})$  with the function `posterior_sampler_gride`. This function is the core of the higher-level routine `bayesfit_gride`. Both take as input `X`, `DM`, `a.d`, `b.d`, `alpha`, `n1`, and `n2`. Moreover, the following inputs can be specified:

- **sigma**: the standard deviation of the proposal for the Metropolis-Hastings step. The default value is set to 0.5;



Dataset	R object	n1	n2	conf_lev	Lower Bound	Estimate	Upper Bound
Swissroll	sw11	1	2	0.95	1.9378	2.0575	2.1825
	sw21	2	4	0.95	1.8252	1.9054	1.9946
	sw31	5	8	0.95	1.8703	1.9406	2.0130
	sw41	5	15	0.95	1.8703	1.9085	1.9485
	sw12	1	2	0.99	1.9001	2.0575	2.2380
	sw22	2	4	0.99	1.8033	1.9054	2.0237
	sw32	5	8	0.99	1.8518	1.9406	2.0337
	sw42	5	15	0.99	1.8590	1.9085	1.9622
Student_T	st11	1	2	0.95	4.5587	4.9660	5.4065
	st21	2	4	0.95	5.0468	5.3758	5.7456
	st31	5	8	0.95	4.7018	4.9532	5.2253
	st41	5	15	0.95	4.8192	4.9565	5.1052
	st12	1	2	0.99	4.4142	4.9660	5.5764
	st22	2	4	0.99	4.9822	5.3758	5.9033
	st32	5	8	0.99	4.6383	4.9532	5.2960
	st42	5	15	0.99	4.7682	4.9565	5.1629

Table 6: MLEs and bootstrap CIs for the `id` obtained with `mle_gride`. Different NN orders and confidence level are used.

- `nsim`: the number of posterior samples to collect;
- `burn_in`: number of discarded initial iterations to allow the chain to reach convergence;
- `start_d`: the user-specified initial value. If `NULL`, the MLE is adopted instead.

The first function returns the posterior MCMC sample. We now show the results according to two different specifications of the standard deviation  $\sigma$  of the proposal distribution for the Metropolis-Hastings algorithm.

```
R> sam1 <- posterior_sampler_gride(X = Swissroll, n1 = 2, n2 = 4)
R> sam2 <- posterior_sampler_gride(X = Swissroll, n1 = 2, n2 = 4, sigma = .1)
```

Figure 9 shows the trace plots of the two chains, obtained by applying the `autoplot` method to the objects returned by `posterior_sampler_gride`. By tuning the parameter `sigma`, different mixing of the chains can be achieved.

Alternatively, we can use the high-level function `bayesfit_gride` to collect a more complete and interpretable output in terms of inference.

```
R> baydot <- bayesfit_gride(X = Swissroll, nsim = 10000, burn_in = 50000,
+                           n1 = 2, n2 = 4, sigma = .1)
```

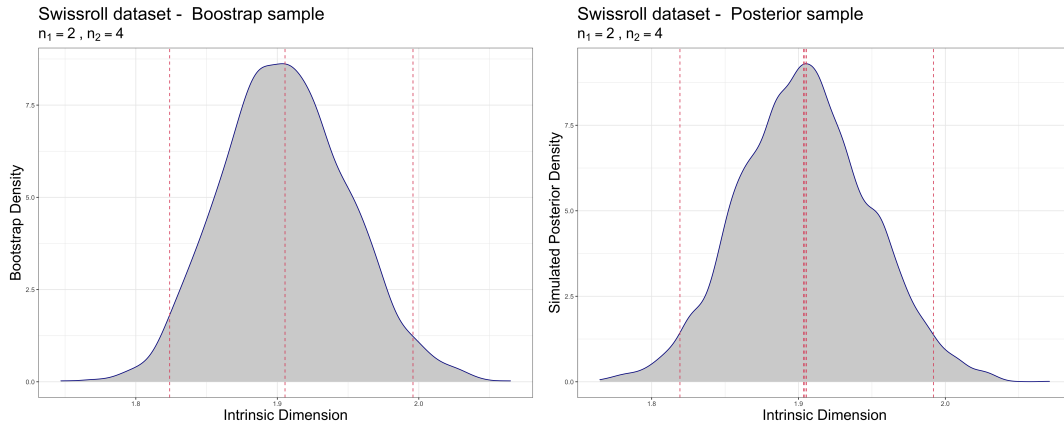


Figure 8: `Swissroll` dataset. The left panel shows the bootstrap density simulated with `bootstrap_gride`. The right panel shows the posterior density simulated with `bayesfit_gride`.

The function returns a list. The principal distributional values that summarize the posterior can be extracted with `baydot$Estimates`. We show the resulting posterior density in the right panel of Figure 8, produced with `autoplot`.

```
R> autoplot(baydot)
R> baydot$Estimates
```

Lower Bound	Mean	Median	Mode	Upper Bound
1.819256	1.904314	1.903480	1.905358	1.991911

### 3.5 Hidalgo: heterogeneous intrinsic dimension estimators

The methods presented so far allow us to determine the `id` of a dataset accurately and efficiently. Given the data generating process of the simulated data, it is easy to compare the obtained estimates with the ground truth for  $\mathcal{D}_1$  and  $\mathcal{D}_2$ . However, the same task is not immediate when dealing with the `GaussMix` table. For  $\mathcal{D}_3$ , it is unclear what `id` value should represent the ground truth. The issue arises because the `GaussMix` data points are generated from Gaussian distributions lying on different manifolds of heterogeneous dimensions.

To introduce the problem, we start by considering the estimates obtained for `GaussMix` with the MLE and the linear fit `TWO-NN` estimators.

```
R> mle_twonn(GaussMix %>% select(-Mix_comp))

      Lower Bound Estimate Upper Bound
[1,]    1.782876 1.875404    1.972805

R> linfit_twonn(GaussMix%>% select(-Mix_comp))
```

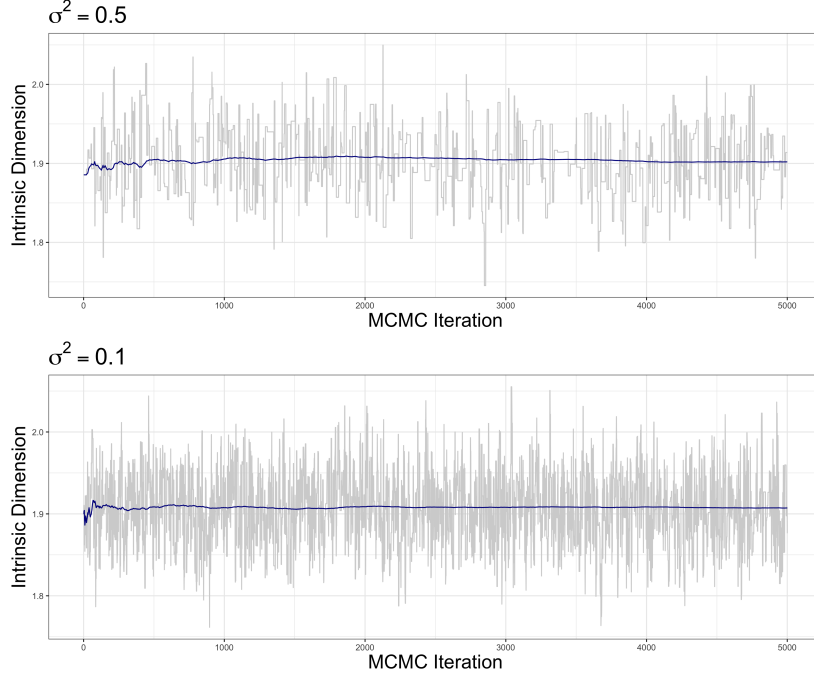


Figure 9: MCMC iterations for the `id` parameter obtained with the function `posterior_sampler_grid`. The top and bottom panel differ for their values of the standard deviation of the proposal distribution.

\$Estimates

Lower Bound	Estimate	Upper Bound
1.433901	1.454059	1.474218

Here, we see that the estimates obtained with the different methods do not agree. Figure 10 raises concerns about the appropriateness of the model. The data points are colored according to their generating mixture component. The log-ratios present a non-linear pattern, where the slope values vary among the different mixture components A, B, and C.

We claim that the methods presented so far are powerful tools for estimating an overall `id` of a dataset, but they all rely on the assumption that the `id` of the data is unique. However, the last example suggests that this hypothesis is limiting and easily violated when dealing with complex data. To address this issue, in Section 2.3 we introduced `Hildalgo`, a Bayesian finite mixture model for heterogeneous `id` estimation. `Hildalgo` addresses the presence of multiple manifolds in the same dataset, yielding a vector of different estimated `id` values  $\mathbf{d}$ . As already discussed, the estimation of a mixture model with Pareto components is challenging. A naive model-based estimation can lead to inaccurate results since there is no clear separation between the kernel densities. Therefore, we modify the classical Bayesian mixture using the likelihood stated in Equation (10). By introducing the extra term  $\prod_{i=1}^n \pi(\mathcal{N}_i^{(q)}|\mathbf{z})$  into the likelihood, we can induce local homogeneity, which helps

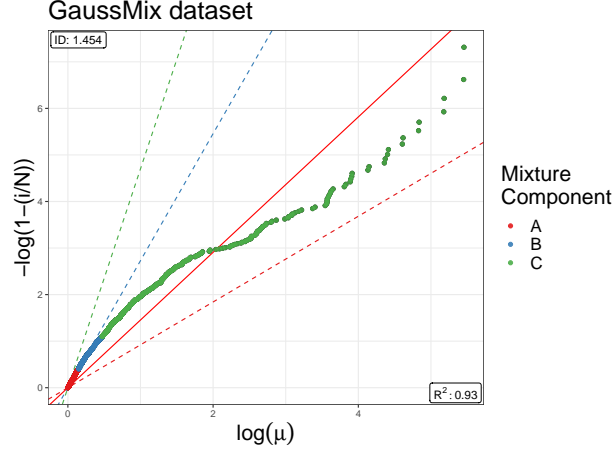


Figure 10: Linear estimator applied to the **GaussMix** dataset. The points are colored according to the mixture component from which they originate. The gray lines represent the linear estimators applied to the subsets of points relative to each mixture component.

identify the model parameters.

Using **intrRinsic**, we can compute the ratios and adjacency matrix needed to evaluate the likelihood from the data points with **Hidalgo\_data\_preprocessing**. This function takes as arguments the dataset **X**, the distance matrix **DM**, and

- **q**: integer, the number of NNs to be considered in the construction of the matrix  $\mathcal{N}^{(q)}$ . Default is 3.

The function returns a list that contains, along with the value of **q** provided as input, the following two objects:

- **mu**: the vector of ratios of distances - easily obtained via **generate\_mus**;
- **Nq**: the binary adjacency matrix.

To provide an idea of the structure of the adjacency matrix  $\mathcal{N}^{(q)}$ , we report three examples obtained from a random sub-sample of the **GaussMix** dataset for increasing values of **q**.

```
R> set.seed(12345)
R> ind <- sort(sample(1:1500, 100, F))
R> DPreP1 <- Hidalgo_data_preprocessing(X = GaussMix[ind, -6], q = 3)
R> DPreP2 <- Hidalgo_data_preprocessing(X = GaussMix[ind, -6], q = 10)
R> DPreP3 <- Hidalgo_data_preprocessing(X = GaussMix[ind, -6], q = 20)
```

We display the heatmaps of the resulting matrices in Figure 11. As **q** increases, the binary matrix becomes more populated, uncovering the neighboring structure of the data points. Allegra et al. [2020] investigated how the performance of the model changes as **q** varies. They suggest fixing **q** = 3, a value that provides a good trade-off between the flexibility of the mixture allocations and local homogeneity.

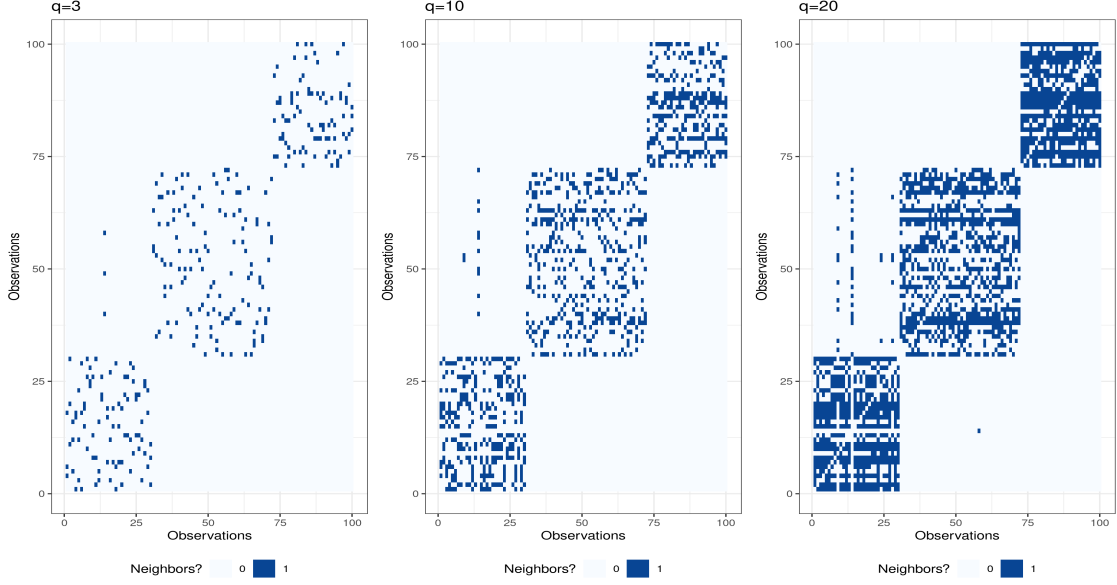


Figure 11: Heatmaps of the adjacency matrices  $\mathcal{N}^{(q)}$  computed on a subset of observations of the **GaussMix** dataset. Different values of  $q$  are assumed.

The core, high-level function to fit the Bayesian mixture is **Hidalgo**. This routine implements the Gibbs sampler described in Section 2.3. The function has the following arguments: **X**, **DM**, **q** and

- **K**: integer, number of mixture components;
- **nsim**, **burn\_in**, and **thinning**: number of MCMC iterations to collect, initial iterations to discard, and thinning interval, respectively;
- **verbose**: logical, should the progress of the sampler be printed;
- **csi**: real between 0 and 1, local homogeneity parameter. Default is 0.75;
- **alpha\_Dirichlet**: parameter of the Dirichlet prior on the mixture weights;
- **a0\_d** and **b0\_d**: shape and rate parameter of the Gamma prior on  $d$ ;
- **prior\_type**: character, type of Gamma prior on  $d$  which can be
  - **Conjugate**: a Gamma prior is adopted;
  - **Truncated**: a truncated Gamma prior on the interval  $(0, D)$ . This is useful for small datasets to avoid the estimated  $id$  exceeding the nominal dimension  $D$ ;
  - **Truncated\_PointMass**: same as **Truncated**, but a point mass is placed on  $D$ . That is, the estimated  $id$  is allowed to be exactly equal to the nominal dimension  $D$ ;
- **D**: integer, the nominal dimension of the dataset;
- **pi\_mass**: probability placed a priori on  $D$  when a **Truncated\_PointMass** prior specification is chosen;

- **recap**: logical, if TRUE the function includes a list of the chosen parameters in the output;
- **if\_coda**: logical, if TRUE the function returns the simulated chains as a `coda` object.

We apply the `Hidalgo` model on the `GaussMix` dataset with two different prior configurations: conjugate and truncated with point mass at  $D = 5$ . The code is the following:

```
R> set.seed(1234)
R> hid_fit <- Hidalgo(X = as.matrix(GaussMix[,-6]), K = 10,
+                      alpha_Dirichlet = 0.05, verbose = F
+                      nsim = 2000, burn_in = 2000)
R> set.seed(1234)
R> hid_fit_TR <- Hidalgo(X = as.matrix(GaussMix[,-6]), K = 10,
+                          prior_type = "Truncated_PointMass",
+                          D = 5, alpha_Dirichlet = 0.05, verbose = F,
+                          nsim = 2000, burn_in = 2000)
```

Notice that, by using `alpha_Dirichlet = 0.05`, we have adopted a sparse mixture modeling approach in the spirit of [Malsiner-Walli et al. \[2016, 2017\]](#).

The output object `hid_fit` is a list of class `Hidalgo`, containing three elements:

- **membership\_labels**: a matrix of dimension `nsim`×`n`. Each column contains the MCMC sample of the membership labels for every observation;
- **cluster\_prob**: a matrix of dimension `nsim`×`L`. Each column contains the MCMC sample of the mixing weight for each mixture component;
- **intrinsic\_dimension**: a matrix of dimension `nsim`×`L`. Each column contains the MCMC sample for the `id` estimated in each cluster.

Selecting `recap = TRUE` adds a list with details of the run to the output. This allows us to collect a summary of all the input values previously specified. For a simple visualization of raw MCMC samples, we can use the function `autoplot`.

```
R> r1 <- autoplot(output = hid_fit) + ggtitle("Conjugate Prior")
R> r2 <- autoplot(output = hid_fit_TR) + ggtitle("Truncated_PointMass Prior")
```

Plotting the trace plots of the elements in  $\mathbf{d}$  allows us to assess the convergence of the algorithm. We need to be aware that the chains may suffer from label-switching issues, which prevent us from drawing inference from the MCMC output directly. Due to the label-switching, mixture components can be discarded and emptied or repopulated across iterations. Figure 12 shows the MCMC trace plots of the two models, with the ergodic means for each mixture component superimposed. Additionally, we can see that if no constraint is imposed on the support of the prior distribution for  $\mathbf{d}$  (left panel), the posterior estimates can exceed the nominal dimension  $D$  of the dataset. This problem disappears when imposing a truncation on the prior support (right panel).

To address the label-switching issue and perform meaningful inference, we need to post-process the results. A simple solution is implemented in the function `Hidalgo.postpr_chains`, which takes as input an object of class `Hidalgo`, along with:

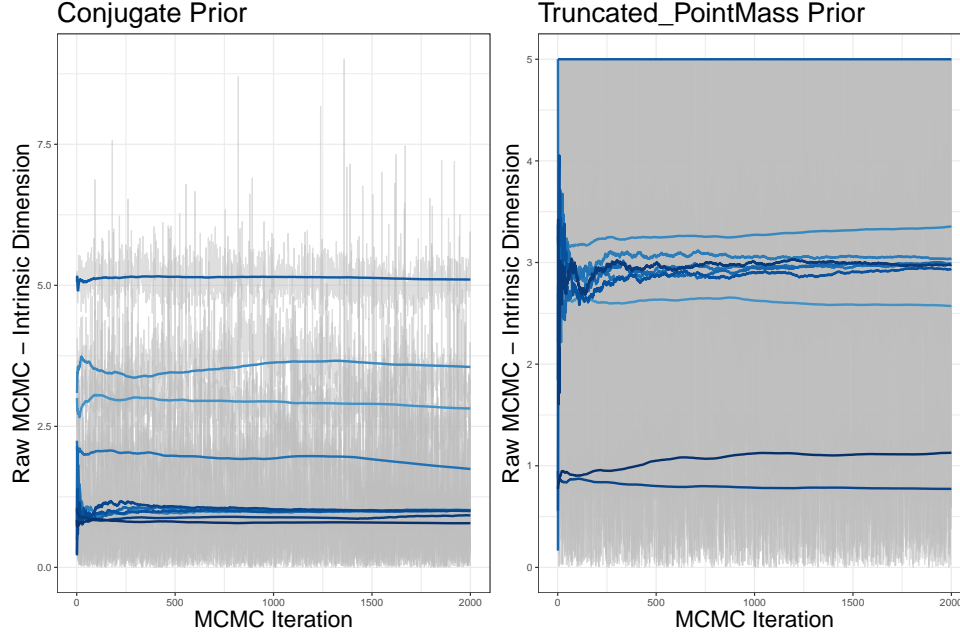


Figure 12: MCMC trace plots and superimposed ergodic means of components of the vector  $\mathbf{d}$ . Left panel: conjugate prior specification. Right panel: truncated with point mass prior specification.

- **all\_chains**: logical, if TRUE all the chains, after the disentanglement for label switching, are reported. If FALSE, a dataset with summary statistics is returned instead.

The post-processing procedure works as follows. Let us consider a MCMC sample of length  $T$ , and denote a particular MCMC iteration with  $t$ ,  $t = 1, \dots, T$ . Let  $z_i(t)$  indicate the cluster membership of observation  $i$  at the  $t$ -th iteration. Similarly,  $d_k(t)$  represents the value of the estimated id in the  $k$ -th mixture component at the  $t$ -th iteration. The function `Hidalgo_postpr_chains` maps the  $K$  chains for the parameters in  $\mathbf{d}$  to each data point via the values of  $\mathbf{z}$ . That is, it constructs  $\mathbf{n}$  chains, one for each observation, by computing  $d_k^*(t) = d_{z_i(t)}(t)$ . We then obtain a collection of chains that link every observation to its id estimate. When the chains have been post-processed, the local observation-specific id can be estimated by the ergodic mean or median.

```
R> post1 <- Hidalgo_postpr_chains(output = hid_fit, all_chains = F)
R> post1_TR <- Hidalgo_postpr_chains(output = hid_fit_TR, all_chains = F)
```

If `all_chains = TRUE`, the function returns a `tibble` of class `hid_all_mcmc`, containing the entire post-processed chains. Otherwise, it returns a `tibble` of class `hid_sum_mcmc` that encompasses summary statistics (mean and principal quantiles) for each observation. For both classes, a suitable `autoplot` method is defined. In this case, we have

```
R> autoplot(post1) + ggtitle("Conjugate Prior")
```

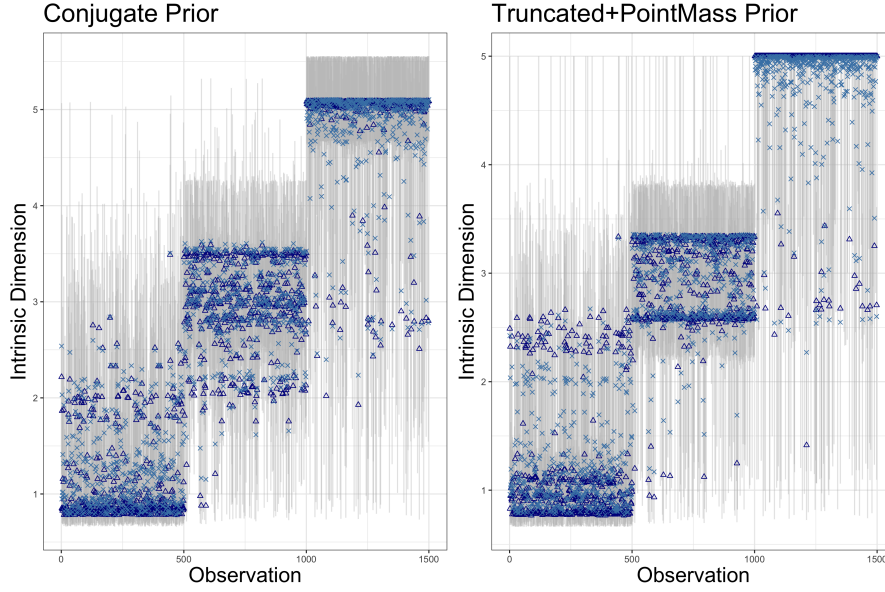


Figure 13: Observation-specific mean and median id represented with black crosses and red triangles, respectively. The gray bars represent a 90% credible interval. The two panels correspond to the two different prior specifications.

```
R> autoplot(post1_TR) + ggtitle("Truncated_PointMass Prior")
R> kable(head(post1$ID_summary))
```

	Q.05	Q.25	MEAN	MEDIAN	Q.75	Q.95	OBS
	-----:	-----:	-----:	-----:	-----:	-----:	----
	1.2083	1.8481	2.5386	2.2175	3.1230	5.0666	1
	0.6989	0.7792	0.9477	0.8518	0.9562	1.4386	2
	0.7652	1.0224	2.0319	1.8650	2.9425	3.9050	3
	0.6901	0.7650	1.0146	0.8439	0.9798	2.2052	4
	0.6832	0.7589	0.9847	0.8265	0.9231	1.9468	5
	0.7404	0.8465	1.4106	1.1572	1.7989	2.9472	6

The created plots are shown in Figure 13. They display the mean (cross) and median (triangle) id estimates for each data point. The separation of the data into the three generating manifolds is evident. Also, we notice that some of the estimates in the conjugate case are incorrectly above the nominal value  $D=5$ , justifying the need for a truncated prior.

Once the observation-specific id chains are computed, we can investigate the presence of potential patterns between the ids and external variables, if available. To explore these possible relations, we can use the function `Hidalgo_ID_class`. Along with an object of class `Hidalgo`, we need to specify:

- `class`: factor, the variable used to stratify the id posterior estimates;



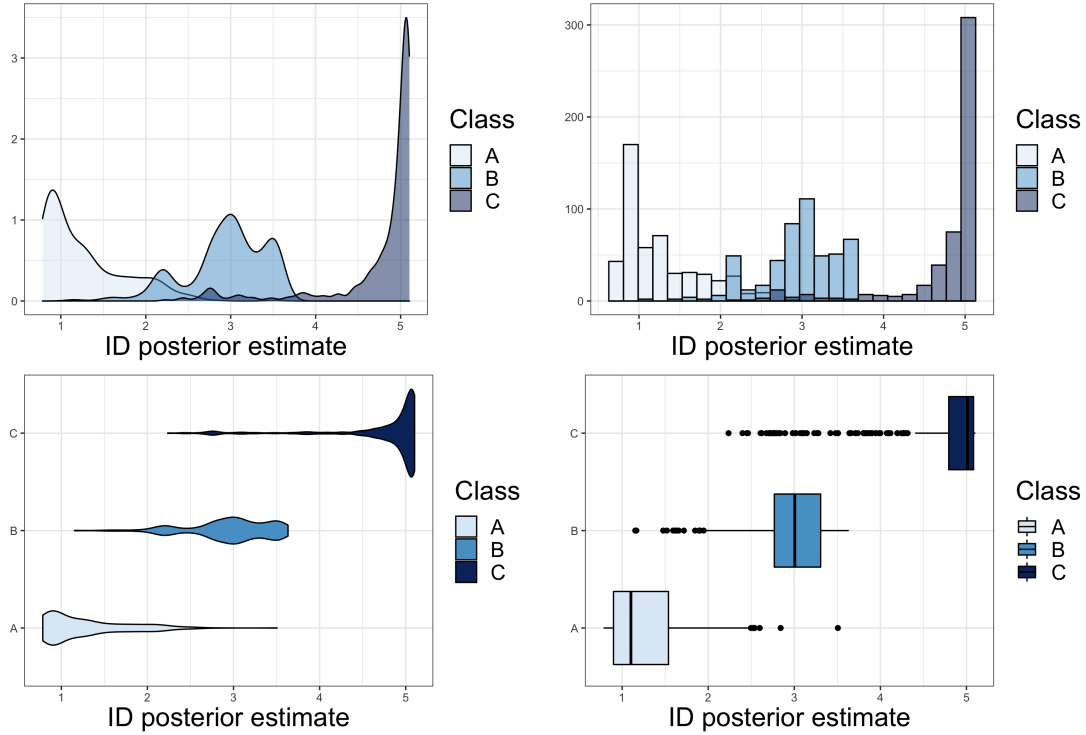


Figure 14: `Hidalgo_ID_class` produces four types of plots. The `ids` estimates of the `GaussMix` dataset are stratified according the generating distribution, as specified in the `class` argument.

- `avg`: logical, if `TRUE` the average is used, if `FALSE`, the median is adopted;

To visualize the results, we can pass the output of this function to `autoplot`. This time, we also need to specify the variable `class` and

- `type`: the type of plot we require. The default is `histogram`. Other possibilities are `density`, `violin`, and `boxplots`.

As an example, Figure 14 shows the four possible plot types, with the `id` estimates of the `GaussMix` dataset stratified by the generating manifold of the observations (passed as `class`).

```
R> mix_comp <- pull(GaussMix[, 6])
R> d1 <- Hidalgo_ID_class( output = hid_fit, class = mix_comp, avg = TRUE )
R> autoplot(d1, class = mix_comp, type = "density")
R> autoplot(d2, class = mix_comp, type = "histogram")
R> autoplot(d3, class = mix_comp, type = "violin")
R> autoplot(d4, class = mix_comp, type = "boxplot")
```

In Bayesian mixture models, the posterior co-clustering matrix (PCM) represents an important source of information. The entries of this matrix are computed as the proportion

of times in which two observations have been clustered together across the MCMC iterations. The PCM provides a description of the underlying clustering structure of the data detected by `Hidalgo`. We can compute the PCM with `Hidalgo_coclustering_matrix`.

Given the PCM, we can compute a variety of widely used loss-functions on the space of the partitions. Examples are the Binder loss [Lau and Green, 2007] or Variation of Information [Wade and Ghahramani, 2015]. By minimizing the loss functions, we can retrieve the optimal partition of the dataset into clusters. The function relies on the functions `minVI` from the R packages `mcclust.ext`. Thus, `Hidalgo_coclustering_matrix` takes as inputs an object of class `Hidalgo` and

- `estimate_clustering`: logical, if TRUE the best partition of the data obtained by minimizing the Variation of Information is estimated;
- `greed`: logical, if TRUE the best partition is recovered adopting a greedy algorithm.

In our case, for example, we can write:

```
R> cl <- factor(pull(GaussMix[,6]))
R> coc <- Hidalgo_coclustering_matrix(output = hid_fit_TR,
+                                     class = cl,
+                                     VI = F, greed = F)
```

We can plot the result using `autoplot`, specifying as inputs the object returned by `Hidalgo_coclustering_matrix`, and possibly `class` (to stratify the rows according to an external variable) and

- `id_names`: a vector of label that uniquely identifies the observations. Default is NULL.

```
R> autoplot(object = coc, class = mix_comp)
```

As we can see from Figure 15, the model correctly detects the three clusters in the data.

### 3.6 Alon dataset: gene microarray measurements

We now apply the functions discussed so far to investigate the `id` of the `Alon` dataset. A copy of this famous microarray measurements table can be accessed via the R package `HiDimDA`. The dataset, first presented in Alon et al. [1999], contains microarray data for 2000 genes measured on 62 patients. Among them, 40 were diagnosed with colon cancer and 22 are healthy subjects. A factor variable named `status`, describes the patient health status. We store the gene measurements in the object `Xalon`, a matrix of nominal dimension  $D=2000$  with  $n=62$  observations. To load the the dataset, write:

```
R> library(HiDimDA)
R> data("AlonDS")
R> status <- factor(AlonDS$grouping, labels = c("Cancer", "Healthy"))
R> Xalon <- as.matrix(AlonDS[, -1])
```

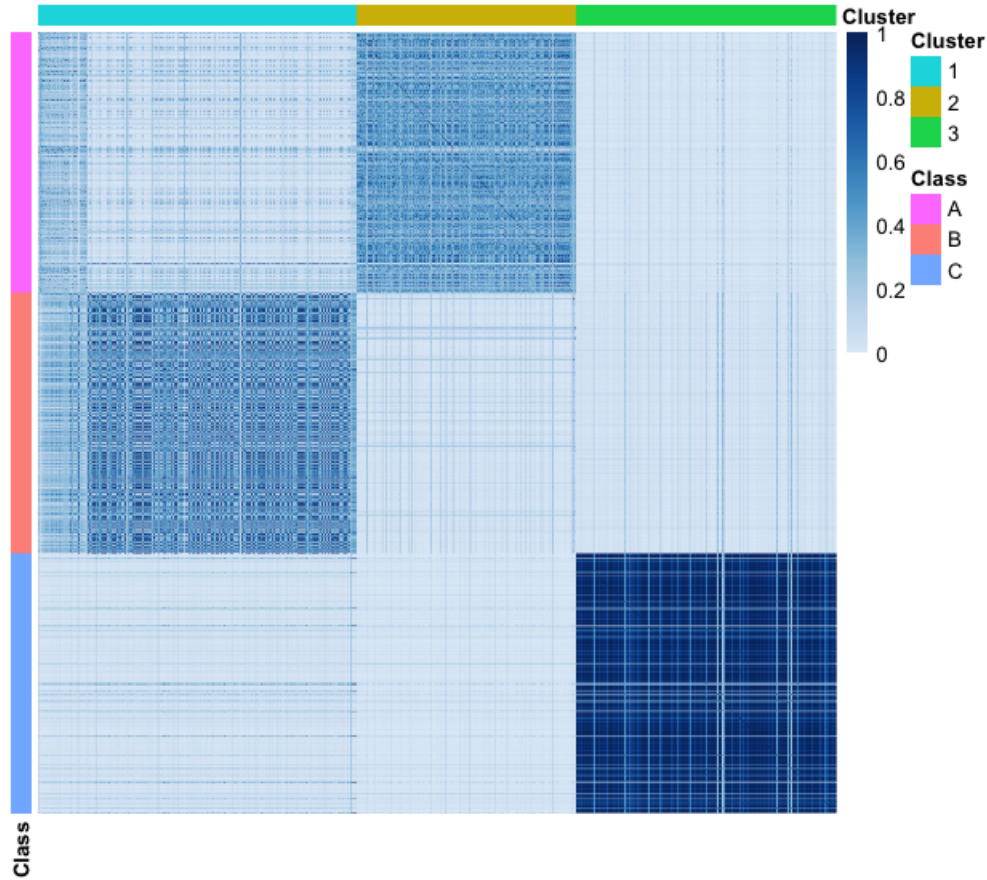


Figure 15: Posterior co-clustering matrix computed from the output of the Hidalgo model. The rows are arranged according to the factor variable `class`, while the columns are sorted according to the best partition found with `minVI` from the package `mcclust.ext`.

We obtain a visual summary of the dataset by plotting the heatmap of the log-data values annotated by `status`. The result is shown in Figure 16.

```
R> Ann <- data.frame("Health Status"=class)
R> rownames(Xalon) <- rownames(Ann) <- paste("Patient",1:62)
R> ann_colors <- list( Health.Status = c(Healthy="blue",Cancer= "lightblue"))
R> pheatmap::pheatmap(log(Xalon), show_colnames = F,
+                       cluster_cols = T, cluster_rows = T,
+                       annotation_row = Ann, angle_col = "0",
+                       annotation_colors = ann_colors )
```

**Homogeneous id.** Let us start with describing the overall complexity of the dataset by computing the estimates assuming a homogeneous id. Using the TWO-NN model, we can compute:

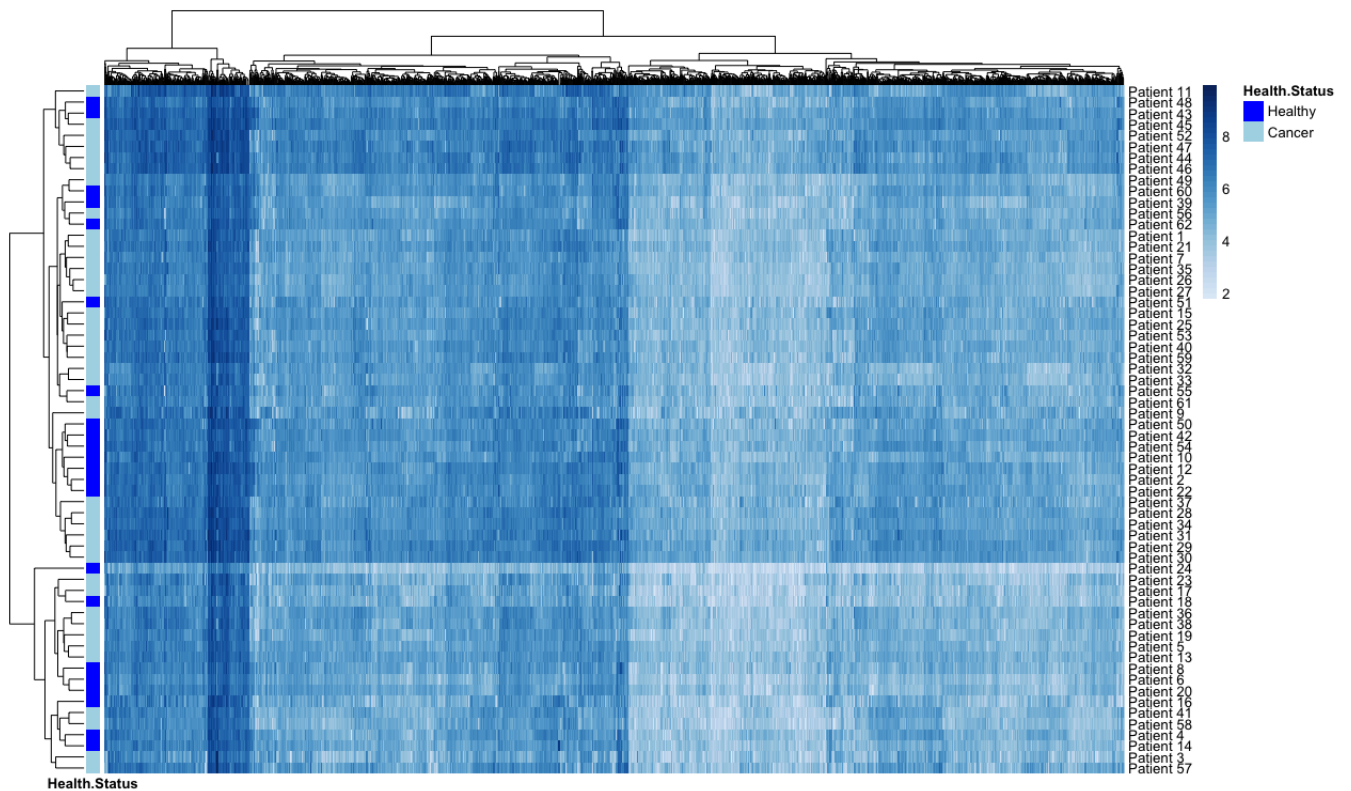


Figure 16: Heatmap of the log values of the Alon microarray dataset. The patients on the rows are stratified according to their health status (Cancer vs Healthy).

```
R> r0 <- mle_twonn(Xalon)
R> r0
```

Lower Bound	Estimate	Upper Bound
7.508059	9.634819	12.37633

```
R> r1 <- linfit_twonn(Xalon)
R> r1$Estimates
```

Lower Bound	Estimate	Upper Bound
9.560248	9.875964	10.191680

```
R> r2 <- bayesfit_twonn(Xalon)
R> r2$Estimates
```

Lower Bound	Mean	Median	Mode	Upper Bound
7.507011	9.791379	9.738788	9.633456	12.374552

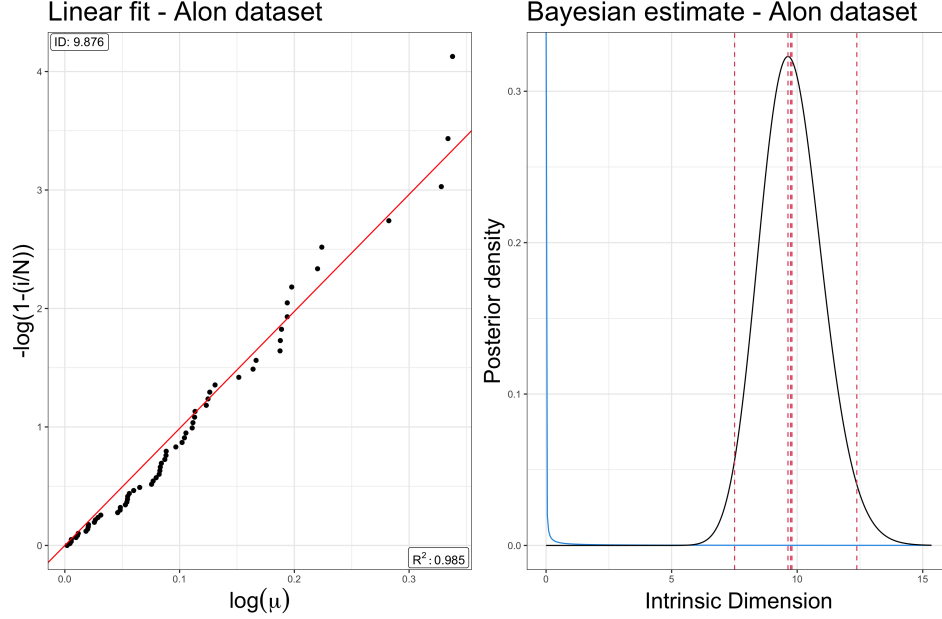


Figure 17: **Alon** dataset. The left panel shows the result of the linear estimator, while the right panel depicts the posterior distribution obtained via the Bayesian approach.

The different estimates based on the **TWO-NN** model agree. The results are also illustrated in Figure 17, which shows the linear fit (left panel) and posterior distribution (right panel). According to these results, we conclude that the information contained in the  $D=2000$  genes can be summarized with approximately ten variables.

**Heterogeneous id.** Alternatively, we can investigate the presence of heterogeneous latent manifolds in the **Alon** dataset by employing **Hidalgo**. Since  $D$  is large, we do not need to truncate the prior on  $d$ . Moreover, given the small number of data points, we opt for an informative prior  $\text{Gamma}(1, 1)$ . We run the model and plot the MCMC sample for the  $\text{id}$  parameter vector  $\mathbf{d}$ .

```
R> set.seed(12345)
R> hid_fit <- Hidalgo(X = Xalon, L = 30, a0_d = 1, b0_d = 1,
+                       alpha_Dirichlet = .05, verbose = F
+                       nsim = 10000, burn_in = 100000, thin=5)
R> autoplot(hid_fit)
```

We see from the ergodic means reported in Figure 18 that we may have incurred the label switching problem: the fluctuations of the highlighted lines suggest that components get selected and discarded during the run. Therefore, we need to post-process our results before drawing any inference.

```
R> post1 <- Hidalgo_postpr_chains(hid_fit, all_chains = F)
```

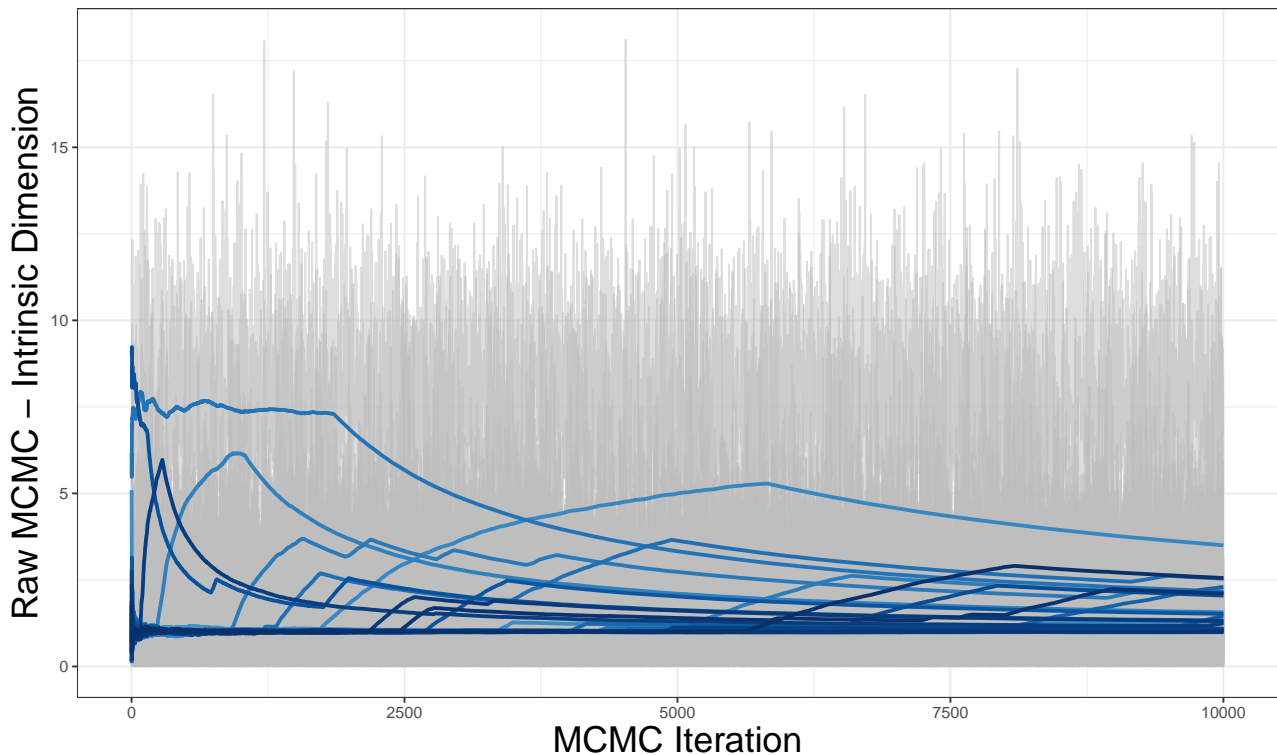


Figure 18: Raw MCMC output of the model `Hidalgo` applied to the `Alon` dataset. The ergodic means of the  $L=30$  mixture components are superimposed. The label switching phenomenon affecting the ergodic means is evident.

As a first step, one should check the PCM. We opt to display the results stratified by `status` and by the optimal estimated partition given the MCMC chains of the cluster membership labels `hid_fit$membership.labels`.

```
R> gr <- Hidalgo_coclustering_matrix(hid_fit, estimate_clustering = T)
R> autoplot(gr, class = status)
```

From the heatmap reported in Figure 19 and the optimal partition found, we conclude that the data can be grouped in two main groups. The next natural step is to investigate how strongly the estimated partition, and in general, the estimated `ids`, are associated with health `status`. As a starting point, we compute the confusion matrix between the optimal partition and `status`:

```
R> table(gr$optimalCL, status)
```

```
status
      Cancer Healthy
1      28      5
```

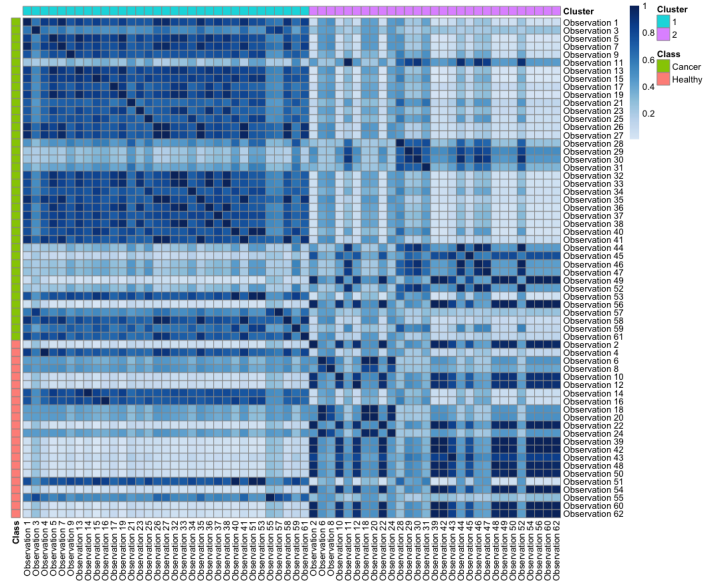


Figure 19: Posterior co-clustering matrix for the Alon dataset. Rows and columns are aggregated according to health **status**, while the columns present the optimal partition.

2      12      17

The estimated partition suggest that there might be an association between health **status** and different values of the **id**. To explore this relation further, we can employ the function `Hidalgo_ID_class`.

```
R> Hidalgo_ID_class(hid_fit, class = status, avg = T)
R> autoplot(d1, type = "boxplot", class = status)
```

We report the boxplots of the posterior **id** means for each subject stratified by **status** in Figure 20. The two groups are characterized by different values of the **id**. This result is remarkable, since it is based only on the topological information of the genes that is enclosed in the distances between NNs.

The estimated individual **id** values are useful to potentially classify the health **status** of new patients according to their genomic profiles. Alternatively, they can be used to train prediction models. As a simple example, we now perform a classification analysis using two **random forest** models, predicting the target variable  $Y = \text{status}$ . To train the models, we use two different sets of covariates: **X\_0**, the original dataset composed of 2000 genes, and **X\_I**, the observation-specific **id** summary returned by `Hidalgo_postpr_ID_chains`.

```
R> X_0 <- data.frame(Y = status, X = Xalon)
R> X_I <- data.frame(Y = status, X = post1$ID_summary[,1:6] )
R> set.seed(12346)
R> rfml <- randomForest::randomForest(Y~.,data=X_0, type="classification")
```

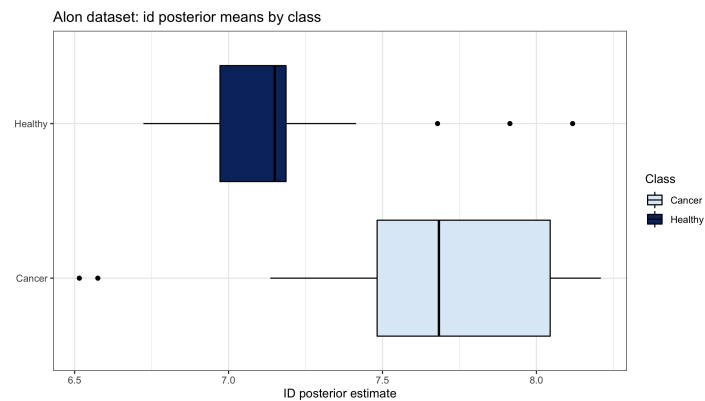


Figure 20: Boxplots of the average individual id values stratified by health status. The healthy group is characterized by values of id that are smaller overall.

```
R> set.seed(12346)
R> rfm2 <- randomForest::randomForest(Y~.,data=X_I, type="classification")
```

We now inspect the results:

```
R> print( rfm1 )
```

Call:

```
randomForest(formula = Y ~ ., data = X_0, type = "classification")
```

Type of random forest: classification

Number of trees: 500

No. of variables tried at each split: 44

OOB estimate of error rate: 19.35%

Confusion matrix:

	Cancer	Healthy	class.error
Cancer	35	5	0.1250000
Healthy	7	15	0.3181818

```
R> print( rfm2 )
```

Call:

```
randomForest(formula = Y ~ ., data = X_I, type = "classification")
```

Type of random forest: classification

Number of trees: 500

No. of variables tried at each split: 2

OOB estimate of error rate: 12.9%

Confusion matrix:



	Cancer	Healthy	class.error
Cancer	36	4	0.1000000
Healthy	4	18	0.1818182

Remarkably, a simple dataset with six variables summarizing the main distributional traits of the observation-specific posterior `ids` obtains better performance in predicting the health `status` than the original dataset. Therefore, we conclude that, in this case, the topological properties of the dataset are associated with the outcome of interest.

The heterogeneous `id` can not only provide a reliable index of complexity for involved data structures, but can also help unveil relationships among data points hidden at the topological level. The application to the `Alon` dataset showcases how reliable `id` estimates represent a fundamental perspective that help us discover hidden data patterns. Furthermore, the extracted information can be subsequently exploited in many downstream analyses such as patient segmentation or predictive analyses.

## 4 Summary and discussion

In this paper we introduced and discussed `intRinsic`, an R package that implements novel routines for the `id` estimation according to the models recently developed in [Facco et al. \[2017\]](#), [Allegra et al. \[2020\]](#), [Denti \[2020\]](#), and [Santos-Fernandez et al. \[2020\]](#). `intRinsic` consists of a collection of high-level, user-friendly functions that in turn rely on efficient, low-level routines implemented in R and C++. We also remark that `intRinsic` integrates functionalities from external packages. For example, all the graphical outputs returned by the functions are built using the well-known package `ggplot2`. Therefore, they are easily customizable using the grammar of graphics [\[Wilkinson, 2005\]](#). Moreover, the MCMC output of the functions implementing the Bayesian models can be exported as `coda` objects.

To summarize, the package includes both frequentist and Bayesian model specifications for the global `id` estimators `TWO-NN` and `Gride`. Moreover, it contains a Gibbs sampler for the posterior simulation of the `Hidalgo` model, which can capture the presence of heterogeneous manifolds within a single dataset. We showed how multiple latent manifolds can help unveil topological traits of a dataset by associating the `id` estimates with external variables. As a general analysis pipeline for practitioners, we suggest starting with the efficient `TWO-NN` functions to understand how appropriate the hypothesis of homogeneity is for the data at hand. If departures from the assumptions are visible, one should rely on `Gride` and `Hidalgo`. The latter also allows exploring the relationship between local `id` estimates and external variables.

The most promising future research directions stem from `Hidalgo`. First, we plan to develop more reliable methods to obtain an optimal partition of the data based on the `id` estimates, since the one proposed heavily relies on a mixture model of overlapping distribution. Moreover, another research avenue worth exploring is a version of `Hidalgo` that relies on the `Gride` distribution, exploiting the information coming from multiple distance ratios that could enhance the `id` estimates. We plan to keep working on this package and to continuously update it in the long run. The novel `id` estimators we discussed

have started a lively research branch, and we intend to include all the future advancements in `intRinsic`.

## 5 Acknowledgements

The author is extremely thankful to Michelle N. Ngo<sup>1</sup>, Derenik Haghverdian<sup>1</sup>, Wendy Rummerfield<sup>1</sup>, Andrea Cappelz<sup>2</sup>, and Riccardo Corradin<sup>2</sup> for their helpful comments and precious insights.

## References

- Michele Allegra, Elena Facco, Francesco Denti, Alessandro Laio, and Antonietta Mira. Data segmentation based on the local intrinsic dimension. *Scientific Reports*, 10(1):1–27, 2020. ISSN 20452322. doi: 10.1038/s41598-020-72222-0. URL <http://arxiv.org/abs/1902.10459>.
- U. Alon, N. Barkai, D. A. Notterman, K. Gish, S. Ybarra, D. Mack, and A. J. Levine. Broad patterns of gene expression revealed by clustering analysis of tumor and normal colon tissues probed by oligonucleotide arrays. *Proceedings of the National Academy of Sciences*, 96(12):6745–6750, 1999. ISSN 0027-8424. doi: 10.1073/pnas.96.12.6745.
- Alessio Ansuini, Alessandro Laio, Jakob H. Macke, and Davide Zoccolan. Intrinsic dimension of data representations in deep neural networks. *Advances in Neural Information Processing Systems*, 32, 2019. ISSN 10495258. URL <http://arxiv.org/abs/1905.12784>.
- Christoph Bartenhagen. *RDRToolbox: A package for nonlinear dimension reduction with Isomap and LLE.*, 2020. R package version 1.38.0.
- Robert S. Bennett. The Intrinsic Dimensionality of Signal Collections. *IEEE Transactions on Information Theory*, 15(5):517–525, 1969. ISSN 15579654. doi: 10.1109/TIT.1969.1054365.
- Alina Beygelzimer, Sham Kakadet, John Langford, Sunil Arya, David Mount, and Shengqiao Li. *FNN: Fast Nearest Neighbor Search Algorithms and Applications*, 2019. URL <https://CRAN.R-project.org/package=FNN>. R package version 1.1.3.
- P. Campadelli, E. Casiraghi, C. Ceruti, and A. Rozza. Intrinsic Dimension Estimation: Relevant Techniques and a Benchmark Framework. *Mathematical Problems in Engineering*, 2015, 2015. ISSN 15635147. doi: 10.1155/2015/759567.
- Robrecht Cannoodt and Wouter Saelens. *dyndimred: Dimensionality Reduction Methods in a Common Format*, 2020. URL <https://CRAN.R-project.org/package=dyndimred>. R package version 1.0.3.

---

<sup>1</sup>University of California, Irvine

<sup>2</sup>University of Milan, Bicocca

- Jose A. Costa and Alfred O. Hero. Geodesic entropic graphs for dimension and entropy estimation in Manifold learning. *IEEE Transactions on Signal Processing*, 52(8):2210–2221, 2004. ISSN 1053587X. doi: 10.1109/TSP.2004.831130.
- Francesco Denti. *Bayesian Mixtures for Large Scale Inference*. PhD thesis, 2020. URL <https://boa.unimib.it/retrieve/handle/10281/262923/382631/phd{ }unimib{ }746944.pdf>.
- Antonio Fabio Di Narzo. *tseriesChaos: Analysis of Nonlinear Time Series*, 2019. URL <https://CRAN.R-project.org/package=tseriesChaos>. R package version 0.1-13.1.
- Dirk Eddelbuettel and Romain François. Rcpp: Seamless R and C++ integration. *Journal of Statistical Software*, 40(8):1–18, 2011. ISSN 15487660. doi: 10.18637/jss.v040.i08.
- Dirk Eddelbuettel and Conrad Sanderson. Rcpparmadillo: Accelerating r with high-performance c++ linear algebra. *Computational Statistics and Data Analysis*, 71:1054–1063, March 2014. URL <http://dx.doi.org/10.1016/j.csda.2013.02.005>.
- Elena Facco and Alessandro Laio. *The intrinsic dimension of biological data landscapes*. PhD thesis, 2017. URL <https://core.ac.uk/download/pdf/144263715.pdf>.
- Elena Facco, Maria D’Errico, Alex Rodriguez, and Alessandro Laio. Estimating the intrinsic dimension of datasets by a minimal neighborhood information. *Scientific Reports*, 7(1):1–8, 2017. ISSN 20452322. doi: 10.1038/s41598-017-11873-y.
- K. Falconer. *Fractal Geometry—Mathematical Foundations and Applications*. John Wiley & Sons, 2nd edition, 2003.
- Constantino A. Garcia. *nonlinearTseries: Nonlinear Time Series Analysis*, 2020. URL <https://CRAN.R-project.org/package=nonlinearTseries>. R package version 0.2.10.
- Jean Golay and Mikhail Kanevski. Unsupervised feature selection based on the Morisita estimator of intrinsic dimension. *Knowledge-Based Systems*, 135:125–134, 2017. ISSN 09507051. doi: 10.1016/j.knosys.2017.08.009.
- Hideitsu Hino. idr: Intrinsic dimension estimation with R. *R Journal*, 9(2):329–341, 2017. ISSN 20734859. doi: 10.32614/rj-2017-054.
- Hideitsu Hino, Jun Fujiki, Shotaro Akaho, and Noboru Murata. Local intrinsic dimension estimation by generalized linear Modeling. *Neural Computation*, 29(7):1838–1878, 2017. ISSN 1530888X. doi: 10.1162/NECO\_a\_00969.
- H. Hotelling. Analysis of a complex of statistical variables into principal components. *Journal of Educational Psychology*, 24(7):498–520, 1933. ISSN 00220663. doi: 10.1037/h0070888.
- Kerstin Johnsson and Lund University. *intrinsicDimension: Intrinsic Dimension Estimation*, 2019. URL <https://CRAN.R-project.org/package=intrinsicDimension>. R package version 1.2.0.

- Ian T. Jolliffe and Jorge Cadima. Principal component analysis: A review and recent developments. *Philosophical Transactions of the Royal Society A: Mathematical, Physical and Engineering Sciences*, 374(2065), 2016. ISSN 1364503X. doi: 10.1098/rsta.2015.0202.
- Olga Kayo. Locally Linear Embedding Algorithm Extensions and Applications. 2006. URL [internal-pdf://isbn9514280415-4255035408/isbn9514280415.pdf](https://doi.org/10.1007/978-1-4020-8415-4).
- J. F. C. Kingman. *Poisson Processes.*, volume 3. 1992. ISBN 0191591246.
- Raivo Kolde. *pheatmap: Pretty Heatmaps*, 2019. URL <https://CRAN.R-project.org/package=pheatmap>. R package version 1.0.12.
- Guido Kraemer, Markus Reichstein, and Miguel D. Mahecha. dimRed and coRanking—unifying dimensionality reduction in r. *The R Journal*, 10(1):342–358, 2018. URL <https://journal.r-project.org/archive/2018/RJ-2018-039/index.html>. coRanking version 0.2.3.
- Jesse H. Krijthe. *Rtsne: T-Distributed Stochastic Neighbor Embedding using Barnes-Hut Implementation*, 2015. URL <https://github.com/jkrijthe/Rtsne>. R package version 0.15.
- John W. Lau and Peter J. Green. Bayesian model-based clustering procedures. *Journal of Computational and Graphical Statistics*, 16(3):526–558, 2007. ISSN 10618600. doi: 10.1198/106186007X238855.
- van der Maaten Laurens and Hinton Geoffrey. Visualizing Data using t-SNE. *Journal of Machine Learning Research*, 9:2579–2605, 2009. ISSN 15729338.
- Elizaveta Levina and Peter J Bickel. Maximum Likelihood Estimation of Intrinsic Dimension. In L K Saul, Y Weiss, and L Bottou, editors, *Advances in Neural Information Processing Systems 17*, pages 777–784. MIT Press, 2005. URL <http://papers.nips.cc/paper/2577-maximum-likelihood-estimation-of-intrinsic-dimension.pdf>.
- Gertraud Malsiner-Walli, Sylvia Frühwirth-Schnatter, and Bettina Grün. Model-based clustering based on sparse finite Gaussian mixtures. *Statistics and Computing*, 26(1-2): 303–324, 2016. ISSN 15731375. doi: 10.1007/s11222-014-9500-2.
- Gertraud Malsiner-Walli, Sylvia Frühwirth-Schnatter, and Bettina Grün. Identifying Mixtures of Mixtures Using Bayesian Estimation. *Journal of Computational and Graphical Statistics*, 26(2):285–295, 2017. ISSN 15372715. doi: 10.1080/10618600.2016.1200472.
- Karl W. Pettis, Thomas A. Bailey, Anil K. Jain, and Richard C. Dubes. An Intrinsic Dimensionality Estimator from Near-Neighbor Information. *IEEE Transactions on Pattern Analysis and Machine Intelligence*, PAMI-1(1):25–37, 1979. ISSN 01628828. doi: 10.1109/TPAMI.1979.4766873.

- Martyn Plummer, Nicky Best, Kate Cowles, and Karen Vines. Coda: Convergence diagnosis and output analysis for mcmc. *R News*, 6(1):7–11, 2006. URL <https://journal.r-project.org/archive/>.
- T. S. Roweis and K. Saul Lawrence. Nonlinear Dimensionality Reduction by Locally Linear Embedding. *Science*, 290:2323–2326, 2000.
- Alessandro Rozza, Gabriele Lombardi, Marco Rosa, Elena Casiraghi, and Paola Campadelli. IDEA: Intrinsic dimension estimation algorithm. *Lecture Notes in Computer Science (including subseries Lecture Notes in Artificial Intelligence and Lecture Notes in Bioinformatics)*, 6978 LNCS(PART 1):433–442, 2011. ISSN 03029743. doi: 10.1007/978-3-642-24085-0\_45.
- Edgar Santos-Fernandez, Francesco Denti, Kerrie Mengersen, and Antonietta Mira. The role of intrinsic dimension in high-resolution player tracking data - Insights in Basketball. *arXiv*, 2020.
- Hana Sevcikova, Don Percival, and Tilmann Gneiting. *fractaldim: Estimation of fractal dimensions*, 2014. URL <https://CRAN.R-project.org/package=fractaldim>. R package version 0.8-4.
- Antonio Pedro Duarte Silva. *HiDimDA: High Dimensional Discriminant Analysis*, 2015. URL <https://CRAN.R-project.org/package=HiDimDA>. R package version 0.2-4.
- J. B. Tenenbaum, V. De Silva, and J. C. Langford. A global geometric framework for nonlinear dimensionality reduction. *Science*, 290(5500):2319–2323, 2000. ISSN 00368075. doi: 10.1126/science.290.5500.2319.
- Sara Wade and Zoubin Ghahramani. Bayesian cluster analysis: Point estimation and credible balls. *arXiv:stat.ME*, 13(2):1–33, 2015. ISSN 19316690. doi: 10.1214/17-BA1073. URL <http://arxiv.org/abs/1505.03339>.
- Hadley Wickham. *ggplot2: Elegant Graphics for Data Analysis*. Springer-Verlag New York, 2016. ISBN 978-3-319-24277-4. URL <https://ggplot2.tidyverse.org>.
- Leland Wilkinson. *The Grammar of Graphics*, volume 95. Springer-Verlag, 2005.
- Kisung You. Rdimtools: An R package for Dimension Reduction and Intrinsic Dimension Estimation. *arXiv*, 2020a.
- Kisung You. *Rdimtools: Dimension Reduction and Estimation Methods*, 2020b. URL <https://CRAN.R-project.org/package=Rdimtools>. R package version 1.0.4.